ORGANOMETALLICS

Article

Cite This: *Organometallics* XXXX, XXX, XXX−XXX

Conceptual Extension of the Degradation−Transformation of N-Heterocyclic Carbenes: Unusual Rearrangements on Osmium

Miguel A. Esteruelas,* M. Pilar Gay, and Enrique Oñate

Departamento de Química Inorgánica, Instituto de Síntesis Química y Catálisis Homogénea (ISQCH), Centro de Innovación en Química Avanzada (ORFEO−CINQA), Universidad de Zaragoza-CSIC, 50009 Zaragoza, Spain

Supporting Information

ABSTRACT: The range of processes of degradation−transformation of NHC ligands in the coordination sphere of a transition metal has been enlarged. The NHC-acyl ligand of the complex Os{κ^2-*C*,*C*-[C(O)CH_2ImMe]}Cl(P^iPr_3)$_2$ (**1**) undergoes a complex rearrangement promoted by internal alkynes to give Os{κ^2-*C*,*N*-[CH_2ImMe]}Cl(CO)(P^iPr_3)$_2$ (**2**). Mechanistic studies have revealed that the degradation involves a catalytic alkyne-mediated deinsertion of CO from the acyl moiety to afford Os{κ^2-*C*,*C*-[CH_2ImMe]}Cl(CO)(P^iPr_3)$_2$ (**3**), followed by a thermally activated stoichiometric 1,2-methylene shift from N to C. The catalytic activity of the alkynes depends upon their substituents, decreasing in the sequence diphenylacetylene > 1-phenyl-1-propyne > 3-hexyne > 2-butyne. Phenylacetylene tautomerizes in the metal coordination sphere to afford the stable vinylidene Os{κ^2-*C*,*C*-[C(O)CH_2ImMe]}Cl(=C=CHPh)(P^iPr_3)$_2$ (**4**), which experiences the coupling of the acyl moiety and the vinylidene ligand under a carbon monoxide atmosphere. The addition of HBF_4·OEt_2 to the resulting complex Os{κ^2-*C*,*C*-[C(=CHPh)C(O)CH_2ImMe]}Cl-(CO)$_2$(P^iPr_3) (**5**) leads to [Os{κ^2-*O*,*C*-[O=C(CH=CHPh)CH_2ImMe]}Cl(CO)$_2$(P^iPr_3)]BF_4 (**6**) containing an NHC-(α,β-unsaturated ketone) ligand.

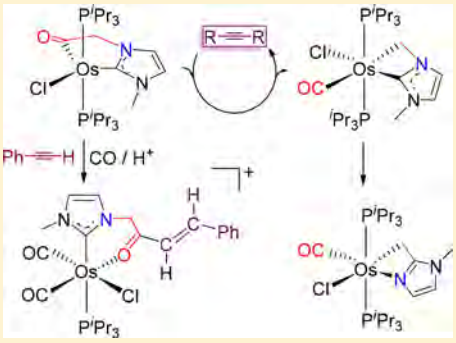

INTRODUCTION

N-heterocyclic carbenes (NHCs) have proven to be very useful ligands in organometallic chemistry and in several of its application fields,[1] particularly in homogeneous catalysis, where they have emerged from the shadow of the phosphines to become primus inter pares.[2] However, a growing number of papers is showing that the N−R arms of some NHC ligands may be involved in intramolecular σ-bond activation reactions,[3] including the cleavage of C−H,[4] C−C,[5] and C−N[6] bonds which gives rise to ligand degradation. These processes have a significant effect on catalysis activation[7] or deactivation.[8] Therefore, their understanding is of fundamental importance to the design of metal catalysts based on these ligands.

Complexes bearing chelating ligands are generally more stable than those only containing monodentate groups. As a consequence, bidentate ligands based on NHC groups have been developed in the search for more robust catalysts.[9] These ligands include neutral bis(NHC) platforms[10] and NHC moieties N-substituted with neutral or anionic sulfur,[11] oxygen,[12] or nitrogen[13] functions. The latter can incorporate hemilability and bifunctionality to their complexes, two properties of great interest in catalysis.[14] One of the characteristics of bifunctional catalysis is that the Brønsted base function interacts with the substrate. Applications of this family of transition-metal−NHC catalysts are continuously appearing,[15] while their degradation pathways have received very scarce attention.

We have recently prepared the five-coordinate complex OsCl{κ^2-*C*,*C*-[C(O)CH_2ImMe]}(P^iPr_3)$_2$ (**1**), which contains a chelated NHC-acyl ligand, by means of the reaction of the hexahydride OsH_6(P^iPr_3)$_2$ with 1-(2-methoxy-2-oxoethyl)-3-methylimidazolium chloride.[16] Its formation involves the direct metalation of the imidazolium moiety, the cleavage of the C−OMe bond of the cation to form methanol, the release of three hydrogen molecules, and the coordination of the anion of the salt to the metal center (Scheme 1). This unsaturated

Scheme 1. Mechanism of Alcoholysis of Pinacolborane with 1

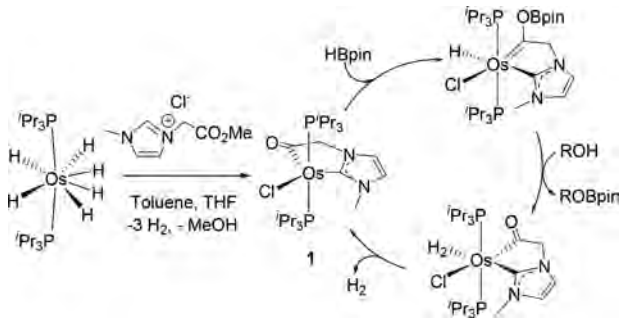

Special Issue: In Honor of the Career of Ernesto Carmona

Received: February 22, 2018

DOI: 10.1021/acs.organomet.8b00110
Organometallics XXXX, XXX, XXX−XXX

compound, which coordinates carbon monoxide, dioxygen, and dihydrogen to form the corresponding adducts, is a bifunctional catalyst for the generation of molecular hydrogen by both the alcoholysis and the hydrolysis of pinacolborane. This ability is a direct consequence of the capacity of the metal center to coordinate small molecules and the acyl oxygen atom to promote heterolytic B−H bond activation.

Alkynes have proven to be useful building blocks in organometallic[17] and organic synthesis.[18] Our interest in knowing the chemical properties of complex **1** prompted us to investigate its behavior in the presence of these hydrocarbons. As a result, we have discovered that the acyl moiety of the NHC-acyl ligand is degraded or transformed into an α,β-unsaturated ketone depending upon the internal or terminal nature of the alkyne. This paper reports the alkyne-mediated degradation of an osmium−NHC complex, its mechanism, and the transformation of a NHC-acyl ligand into NHC-(α,β-unsaturated ketone) in the osmium coordination sphere.

RESULTS AND DISCUSSION

Degradation of the NHC-Acyl Ligand of 1 Mediated by Internal Alkynes. The five-coordinate complex **1** is unstable in the presence of diphenylacetylene. Treatment of its toluene solutions with 4.0 equiv of the hydrocarbon, at 100 °C, for 24 h leads to Os{κ^2-*C*,*N*-[CH_2ImMe]}Cl(CO)(P^iPr_3)$_2$ (**2**) in 65% yield (eq 1). This compound does not contain the

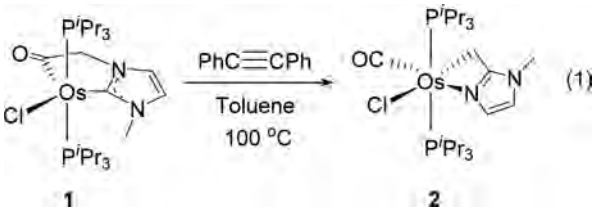

alkyne or any fragment derived from it. Its formation, which is the result of a complex rearrangement in the NHC-acyl ligand, involves the decarbonylation of the acyl group, a 1,2-methylene shift from a N atom to the carbenic-C atom, and the coordination of the free N atom. Under the same conditions, in the absence of alkyne, complex **1** is stable. After 24 h, in toluene, at 100 °C, it is recovered in almost quantitative yield, demonstrating that the hydrocarbon is necessary for the rearrangement.

Complex **2** was isolated as colorless crystals and characterized by X-ray diffraction analysis. Figure 1 gives a view of the structure, which proves the rearrangement and the formation of the new C,N-chelate ligand. The coordination geometry around the osmium atom can be rationalized as a distorted octahedron with trans phosphines (P(1)−Os−P(2) = 175.00(3)°). The perpendicular plane is formed by the chelate ligand, which acts with a C(1)−Os−N(2) bite angle of 64.44(14)°, the chloride anion disposed trans to C(1) (Cl−Os−C(1) = 160.83(11)°), and the carbonyl group located trans to N(2) (C(24)−Os−N(2) = 161.42(15)°). The Os−C(1) bond length of 2.155(4) Å compares well with those reported for other Os−C(sp^3) bonds.[19] In agreement with the presence of this bond in the complex, its ^{1}H NMR spectrum, in dichloromethane-d_2, at room temperature shows the AA′ part of an AA′XX′ spin system centered at 2.27 ppm, for the CH_2 group of the chelate ligand. In the ^{13}C{^{1}H} NMR spectrum, this group displays a triplet ($^2J_{C-P}$ = 4.8 Hz) in the high-field region, at −31.5 ppm. The ^{31}P{^{1}H} NMR spectrum contains a singlet at 3.5 ppm, as

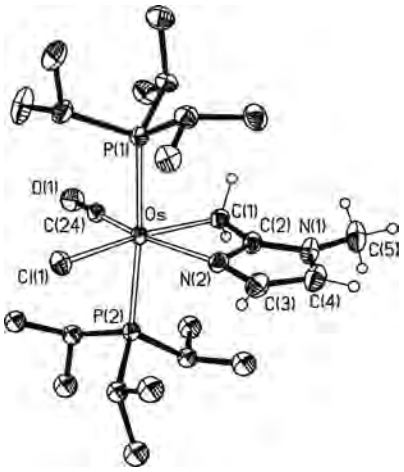

Figure 1. Molecular diagram of complex **2** (50% probability ellipsoids). Most hydrogen atoms are omitted for clarity. Selected bond lengths (Å) and angles (deg): Os−Cl(1) 2.5044(10), Os−P(1) 2.4082(11), Os−P(2) 2.4244(11), Os−N(2) 2.225(3), Os−C(1) 2.155(4), Os−C(24) 1.823(4); P(1)−Os−P(2) 175.00(3), Cl(1)−Os−C(1) 160.83(11), N(2)−Os−C(24) 161.42(15), N(2)−Os−C(1) 64.44(14).

expected for equivalent phosphines. A ν(CO) band at 1870 cm^{-1} in the IR spectrum is also a characteristic feature of this species.

To gain insight into the rearrangement from **1** to **2**, the transformation in toluene was followed by ^{31}P{^{1}H} NMR spectroscopy over 3 days. Figure 2 shows the composition of the mixture as a function of the time, when 3.0 equiv of hydrocarbon per equivalent of complex **1** was used at 70 °C. According to that observed, the formation of **2** (purple ×) takes place via an intermediate **3** (red ■), which reaches a maximun, after about 10 h. The presence of a minor species **3a** (green ▲) and traces of free triisopropylphosphine were also detected.

Intermediate **3** was isolated as an analytically pure white solid from the mixture, when its concentration was maximum, and fully characterized, including X-ray diffraction analysis. The structure has two chemically equivalent but crystallographically independent molecules in the asymmetric unit. Figure 3 shows one of them. The molecules correspond to the species Os{κ^2-*C*,*C*-[CH_2ImMe]}Cl(CO)(P^iPr_3)$_2$ resulting from the deinsertion of the carbonyl group from the acyl, previous to the 1,2-methylene shift. A noticeable feature of its octahedral stereochemistry is the mutually trans disposition of the carbonyl ligand and the methylene group (C(2)−Os−C(25) = 160.78(18) and 160.36(17)°). Because the deinsertion of a carbonyl group is a concerted process, which should lead to the cis disposition of both resulting fragments, this suggests that after the deinsertion an isomerization process takes place. The isomerization should occur via a five-coordinate species, which is consistent with the presence of traces of free phosphine in the course of the rearrangement. The plane perpendicular to the C(2)−Os−C(25) direction is formed by the phosphines disposed mutually trans (P(1)−Os−P(2) = 172.33(4) and 171.77(4)°) and the chloride anion and the imidazolylidene group also disposed mutually trans (Cl−Os−C(1) = 161.77(12) and 161.88(13)°). The Os−methylene distances of 2.273(4) and 2.277(4) Å (Os−C(2)) are about 0.12 Å longer than that of **2**, although the bite angles of the chelate ligand (C(1)−Os−C(2) = 63.01(16) and 63.11(16)°) are

DOI: 10.1021/acs.organomet.8b00110
Organometallics XXXX, XXX, XXX−XXX

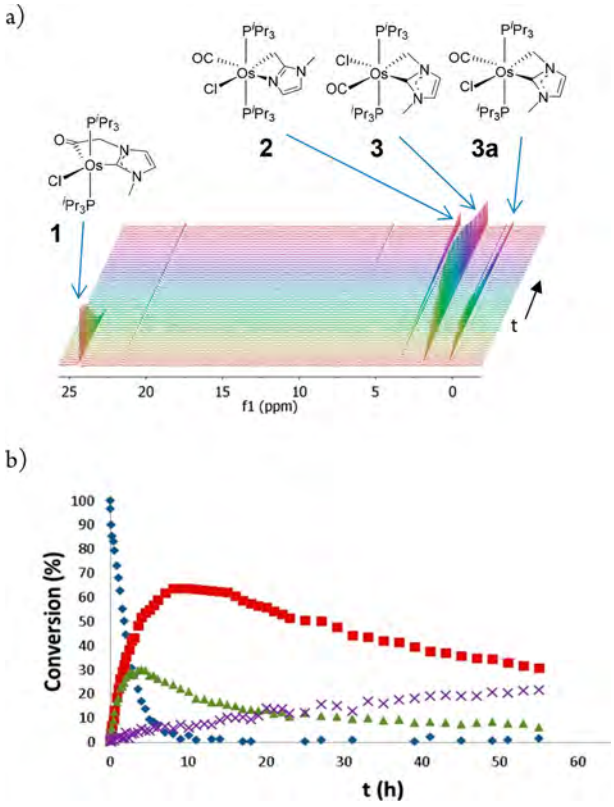

Figure 2. Rearrangement of **1** (blue ◆) into **2** (purple ×), via **3** (red ■) and **3a** (green ▲) promoted by diphenylacetylene as a function of the time, in toluene, at 70 °C: (a) stacked $^{31}P\{^1H\}$NMR spectra; (b) conversion versus time representation.

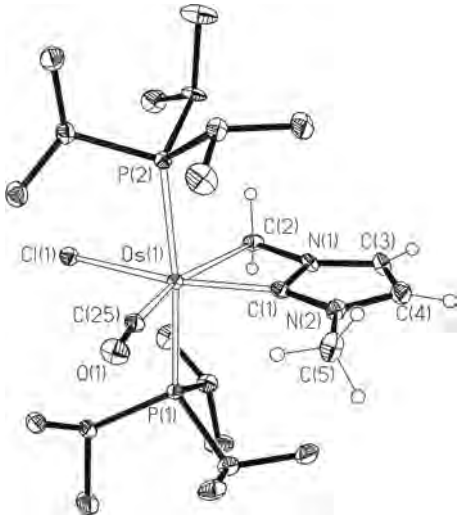

Figure 3. Molecular diagram of complex **3** (50% probability ellipsoids). Most hydrogen atoms are omitted for clarity. Selected bond lengths (Å) and angles (deg): Os(1)−Cl(1) 2.5103(11)/ 2.5081(11), Os(1)−P(1) 2.4158(11)/ 2.4210(11), Os(1)−P(2) 2.4189(11)/2.4168(11), Os(1)−C(1) 2.022(4)/2.029(4), Os(1)−C(2) 2.273(4)/2.277(4), Os(1)−C(25) 1.867(4)/1.870(5); P(1)−Os(1)−P(2) 172.33(4)/171.77(4), Cl(1)−Os(1)−C(1) 161.77(12)/ 161.88(13), C(2)−Os(1)−C(25) 160.78(18)/160.36(17), C(1)−Os(1)−C(2) 63.01(16)/63.11(16).

similar to that of **2**. The Os−C(1) bond lengths of 2.022(4) and 2.029(4) Å compare well with the distances reported for other Os−imidazolylidene derivatives with normal coordination of the NHC.[20] The ^1H, $^{13}C\{^1H\}$, and $^{31}P\{^1H\}$ NMR spectra of **3**, in benzene-d_6 at room temperature, are consistent with the structure shown in Figure 3. The ^1H NMR spectrum shows the methylene resonance at 3.46 ppm as the AA′ part of an AA′XX′ spin system. In the $^{13}C\{^1H\}$ NMR spectrum, this group displays a triplet ($^2J_{C-P}$ = 8.7 Hz) at 17.3 ppm, whereas the signal corresponding to the metalated carbon atom of the imidazolylidene moiety appears at 141.6 ppm (t, $^2J_{C-P}$ = 6.9 Hz). The $^{31}P\{^1H\}$ NMR spectrum shows a singlet at 2.1 ppm for the equivalent phosphines. In agreement with the presence of the carbonyl ligand, the IR contains a ν(CO) band at 1870 cm^{-1}.

Once we obtained the spectroscopic features of **2** and **3**, we deduced the nature and the structure of the minor species **3a** from the ^1H, $^{13}C\{^1H\}$, and $^{31}P\{^1H\}$ NMR spectra of the reaction mixtures enriched in this compound. Complex **3a** is a cis carbonyl methylene isomer of **3**. In accordance with this, the ^1H NMR spectra contain the AA′ part of an AA′XX′ spin system centered at 3.72 ppm, corresponding to the methylene group, the $^{13}C\{^1H\}$ NMR spectra show triplets at 193.1 ppm ($^2J_{C-P}$ = 12.1 Hz), 155.2 ppm ($^2J_{C-P}$ = 11.3 Hz), and −3.8 ppm ($^2J_{C-P}$ = 5.3 Hz) due to the carbonyl ligand, the metalated carbon atom of the imidazolylidene moiety, and the methylene group, respectively, and the $^{31}P\{^1H\}$ NMR spectra contain a singlet at 0.0 ppm for the equivalent phosphines.

The course of the reaction shown in eq 1 depends upon the added amount of diphenylacetylene, increasing its rate as the concentration of alkyne is increased, as expected for an alkyne-mediated process. Figure 4 shows the amount of products formed after 1 h, in toluene, at 80 °C as a function of the added diphenylacetylene.

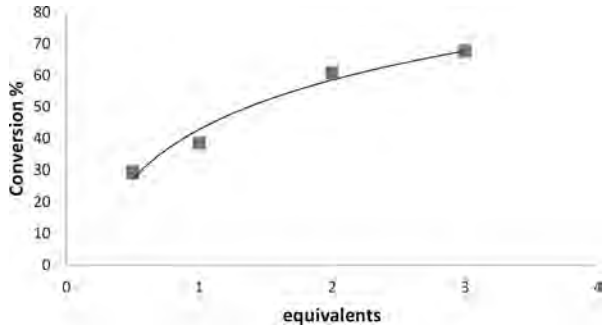

Figure 4. Dependence of the amount of products formed upon the added diphenylacetylene, 1 h in toluene, at 80 °C.

1-Phenyl-1-propyne, 3-hexyne, and 2-butyne also promote the skeletal isomerization. Figure 5 shows the percentage of complex **1** transformed into products after 23 h, in toluene at 70 °C, for the studied alkynes. The reduction of the activity in the sequence diphenylacetylene > 1-phenyl-1-propyne > 3-hexyne > 2-butyne reveals that the efficiency of the alkyne depends upon its substituents, decreasing as the phenyl groups are replaced by alkyl groups and as the steric requirement of the alkyl substituents also decreased. This indicates that both the electronic properties of the triple bond and the bulkiness of the substituents are relevant for the development of the isomerization process.

The availability of **3** allowed us to separately study the 1,2-methylene shift in the presence and in the absence of alkyne, by $^{31}P\{^1H\}$ NMR spectroscopy. The same results were obtained in

DOI: 10.1021/acs.organomet.8b00110
Organometallics XXXX, XXX, XXX−XXX

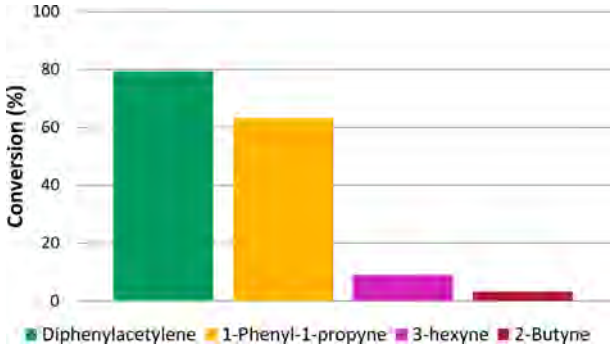

Figure 5. Percentage of formed products after 23 h, in toluene at 70 °C, as a function of alkyne.

both cases, indicating that the shift is not an alkyne-promoted transformation but a thermally activated stoichiometric process. During the isomerization the presence of small amounts of **3a** was detected (Figure 6), which is consistent with a migration occurring in the inner sphere of the metal through five-coordinate species resulting from phosphine dissociation.

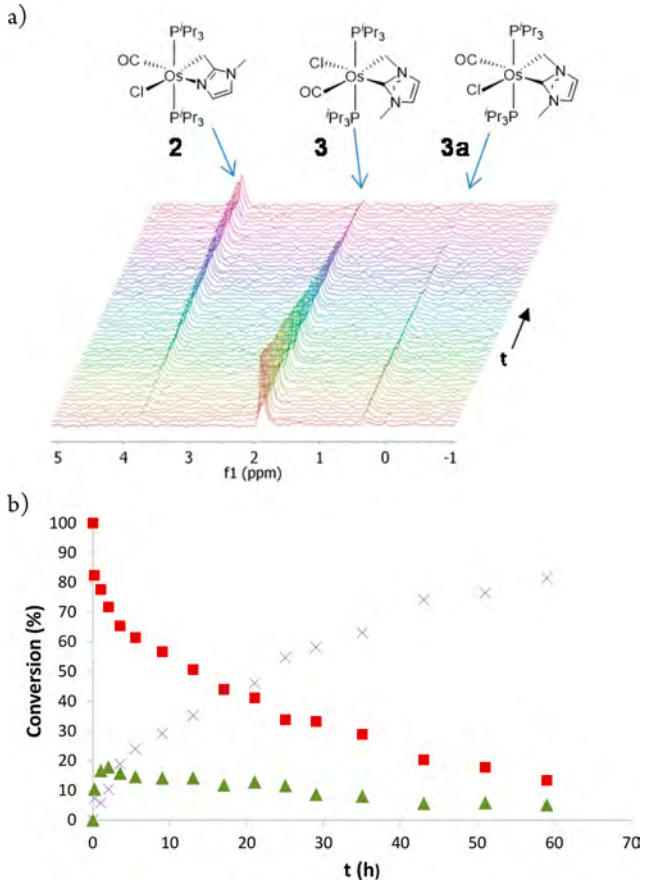

Figure 6. Transformation from **3** (red ■) to **2** (purple ×) and **3a** (green ▲) in toluene at 90 °C as a function of the time: (a) stacked $^{31}P\{^{1}H\}$ NMR spectra; (b) conversion versus time representation.

A catalyst is an atom, ion, molecule, or solid surface which is introduced inside a reaction to diminish the activation energy of the process without affecting the equilibrium constant. The additive offers an alternative path which is energetically much more favored. As a consequence, the rate of the catalyzed process is much faster than that of the uncatalyzed process.[21] The catalyst is usually employed in a substoichiometric amount, although this is not a requirement and reactions using a stoichiometric amount or excess catalyst are known.[22] Thus, from a conceptual point of view, the skeletal isomerization of **1** to **2** promoted by internal alkynes can be rationalized as a tandem process involving the catalytic deinsertion of the carbonyl group from the acyl function of the chelate ligands of **1** to afford **3** and a stoichiometric 1,2-methylene shift in the latter to give **2** (Scheme 2).

Scheme 2. Sequence of Formation of 2 and 3

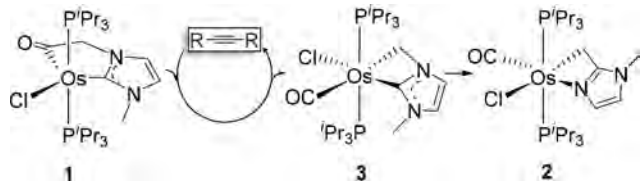

Organometallic catalysis uses a transition-metal complex as catalyst and proceeds through organometallic intermediates,[23] whereas organocatalysis uses a small organic molecule as catalyst and takes place through organic intermediates without the participation of any metal.[24] The combination of organometallic catalysis and organocatalysis is characterized by the use of two different catalysts in the same reaction, one of them purely organic and another metallic.[25] Notable examples of this class of catalysis include Catellani-type reactions, which combine palladium as an inorganic catalyst and a strained olefin such as norbornene as an organic catalyst to form biphenyl derivatives by cross-coupling of aryl halides[26] or to promote *m*-CH alkylation of anilines and phenols[27] or the cross-coupling between Grignard reagents and alkyl halides catalyzed by copper and 1,3-butadiene[28] or 1-phenylpropyne.[29] The transformation of **1** into **3** does not fit into any of these classes of catalysis. It takes place via organometallic intermediates, but it is promoted by a small organic molecule as a unique catalyst.

Mechanism of the Degradation. To gain mechanistic insight about the transformation of **1** into **2**, we have carried out DFT calculations (B3LYP(GD3)//SDD(f)/6-31G**) on both reactions: the CO deinsertion and the 1,2-methylene shift. The changes in free energy (ΔG) were tabulated in toluene at 70 °C.

Scheme 3 shows a catalytic cycle for the acyl decarbonylation reaction, which is consistent with the experimental observations and contextualizes the DFT results, whereas Figure 7 summarizes the energy profile of the catalysis. The coordination of the alkyne to the osmium atom of **1** affords the six-coordinate intermediate **A**, which is 25.4 kcal mol^{-1} less stable than **1** plus diphenylacetylene. The low stability of this species explains why an excess of catalyst is necessary to perform the process with a significant rate. Once this intermediate is formed, the dissociation of a phosphine from the metal center takes place to give the five-coordinate species **B**. The dissociation produces a noticeable stabilization, as a consequence of the reduction of the steric hindrance experienced by the coordinated ligands, while the electron deficiency of the metal center can be compensated by the alkyne ability to act as a four-electron donor.[30] The five-coordinate character of **B** allows the existence of isomers of this species close in energy. Complex **B** is the key intermediate of the reaction, on which the deinsertion occurs. The decarbonylation of the acyl group is

DOI: 10.1021/acs.organomet.8b00110
Organometallics XXXX, XXX, XXX−XXX

Scheme 3. Cycle for the Acyl Decarbonylation of 1 Catalyzed by Internal Alkynes

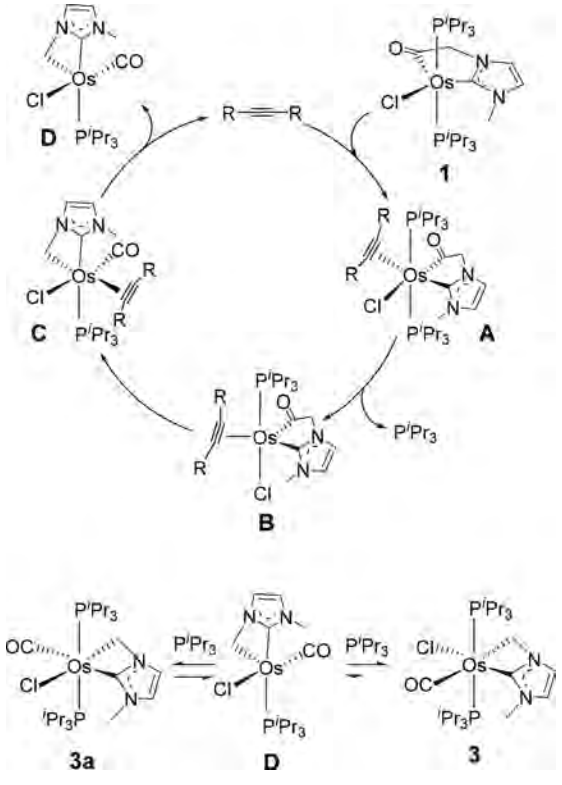

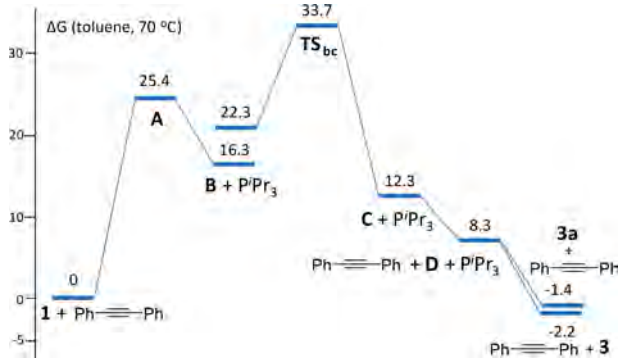

Figure 7. Energy profile (ΔG in kcal mol^{-1}) of the catalysis. The energy of **1** + diphenylacetylene has been taken as a reference.

the determining step of the catalysis and, in agreement with the experimental observations, increases its activation energy in the sequence diphenylacetylene (33.7 kcal mol^{-1}) < 1-phenyl-1-propyne (36.0 kcal mol^{-1}) < 2-butyne (45.1 kcal mol^{-1}). The deinsertion leads to the six-coordinate intermediate **C**, which dissociates the alkyne to give **D** and regenerates the catalyst. The coordination of the dissociated phosphine to **D** yields **3** and **3a**, which are respectively 2.2 and 1.4 kcal mol^{-1} more stable than **1**. Although the contraction of the CMC-metallacycle from five to four members would diminish the stability of **3** and **3a**, the decrease is compensated by the increase associated with the saturated character of the metal center.

The 1,2-hydrogen shift between N and C in NHC ligands bearing a NH wingtip is a well studied exchange.[31] However, the analogous 1,2-carbon shifts are rare. Song and co-workers have very recently reported a rearrangement of a picolyl-functionalized NHC ligand from N,C-chelate to N,N-chelate in Fe(II) and Ru(II) complexes.[32] Experimental and computational studies suggest an intermediate featuring a four-membered CMC metallaring similar to that of **3**. Scheme 4

Scheme 4. Thermal Rearrangement of 3 into 2

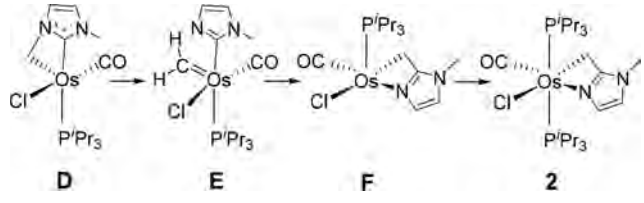

summarizes the stages for the thermal rearrangement of the latter into **2**, starting from intermediate **D**, which is a common species for the geometrical isomerization between **3** and **3a** and for the isomerization by 1,2-methylene shift, once the deinsertion of the carbonyl group has taken place. Figure 8

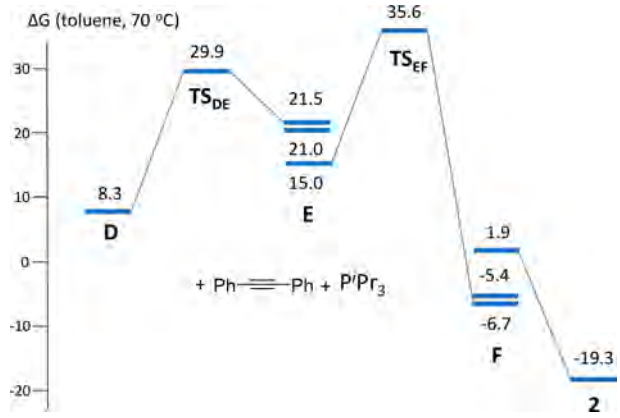

Figure 8. Energy profile (ΔG in kcal mol^{-1}) of the catalysis. The energy of **1** + diphenylacetylene has been taken as a reference.

collects the energy profile for the migration. Complex **D** undergoes the rupture of the N−methylene bond to afford the 2-imidazolyl-alkylidene intermediate **E**, which experiences a double migration in one pot. The metalated carbon atom of the heterocycle is shifted from the metal center to the alkylidene, whereas the free nitrogen atom coordinates to the metal center. This double migration, which leads to **F**, is the rate-determining step for the 1,2-methylene shift. The activation barrier of 35.6 kcal mol^{-1} with regard to **1** plus diphenylacetylene is 1.9 kcal mol^{-1} higher than that for the deinsertion. The coordination of dissociated phosphine to **F** yields **2**.

Transformation From NHC-acyl to NHC-(α,β-unsaturated ketone). In contrast to internal alkynes, phenylacetylene couples with the acyl substituent to finally afford a NHC-(α,β-unsaturated ketone) ligand through a carbon monoxide promoted process, which further involves the addition of a proton (Scheme 5).

Terminal alkynes show a marked inclination to undergo tautomerization into the vinylidene form when they coordinate to unsaturated transition-metal complexes.[33] In agreement with this, the addition of 1.1 equiv of phenylacetylene to acetone solutions of **1** leads to the six-coordinate vinylidene derivative OsCl{κ^2-*C*,*C*-[C(O)CH$_2$ImMe]}(=C=CHPh)(P^{i}Pr$_3$)$_2$ (**4**), after 1 h, at room temperature. Complex **4** was isolated as pink crystals in 66% yield and characterized by X-ray diffraction

DOI: 10.1021/acs.organomet.8b00110
Organometallics XXXX, XXX, XXX−XXX

Scheme 5. Formation of 4, 5, and 6a,b from 1

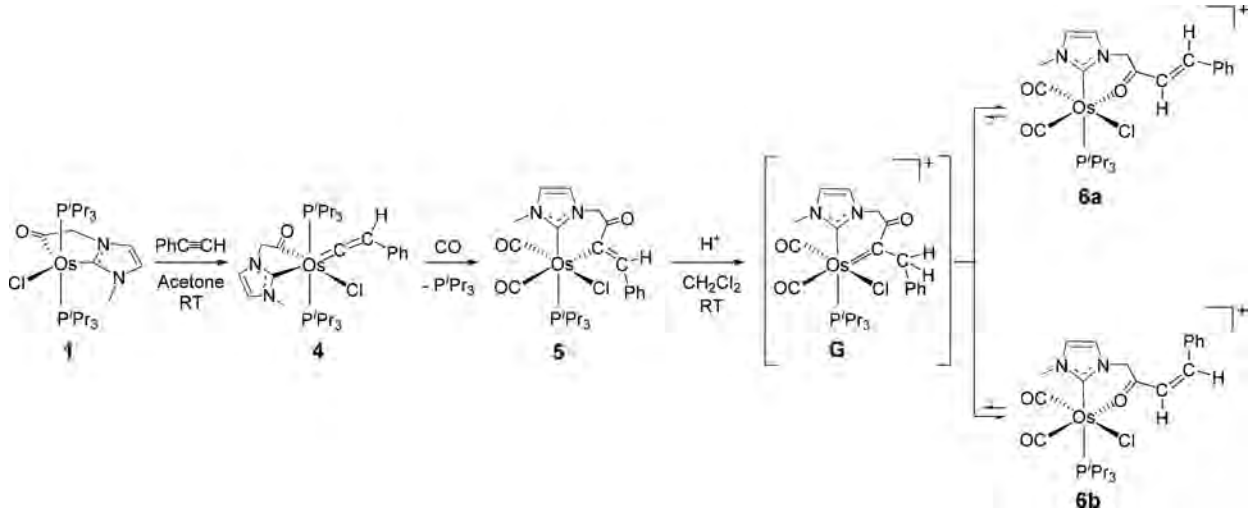

analysis. Figure 9 shows a view of the structure. The coordination geometry around the osmium atom can be

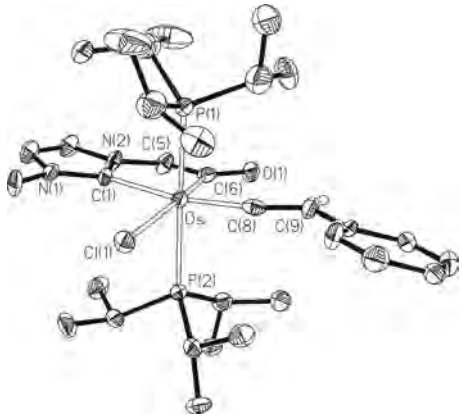

Figure 9. Molecular diagram of complex **4** (50% probability ellipsoids). Most hydrogen atoms are omitted for clarity. Selected bond lengths (Å) and angles (deg): Os−Cl(1) 2.487(2), Os−P(1) 2.435(2), Os−P(2) 2.438(2), Os−C(1) 2.186(8), Os−C(6) 2.031(9), Os−C(8) 1.841(10), C(8)−C(9) 1.343(13); P(1)−Os−P(2) 172.38(8), Cl(1)−Os−C(6) 166.8(3), C(1)−Os−C(8) 164.8(3), C(1)−Os−C(6) 78.4(3), Os−C(8)−C(9) 167.7(8).

rationalized as a distorted octahedron with the phosphine ligands occupying trans positions (P(1)−Os−P(2) = 172.38(8)°). The vinylidene ligand lies on the perpendicular plane disposed trans to the imidazolylidene moiety (C(8)−Os−C(1) = 164.8(3)°), whereas the acyl group is situated trans to the chloride anion (C(6)−Os−Cl(1) = 166.8(3)°). The vinylidene ligand is bound to the metal center in a nearly linear fashion with an Os−C(8)−C(9) angle of 167.7(8)°. The Os−C(8) and C(8)−C(9) bond lengths of 1.841(10) and 1.343(13) Å, respectively, compare well with those found in other osmium−vinylidene complexes.[34] The NHC-acyl ligand coordinates with a C(1)−Os−C(6) bite angle of 78.4(3)° and Os−imidazolylidene and Os−acyl bond lengths of 2.186(8) Å (Os−C(1)) and 2.031(9) Å (Os−C(6)), respectively.

The ^{1}H, ^{13}C{^{31}P}, and ^{31}P{^{1}H} NMR spectra of the isolated crystals, in benzene-d_6, at room temperature are consistent with the structure shown in Figure 9. In the ^{1}H NMR spectrum, the most noticeable feature is the C$_\beta$H resonance of the vinylidene ligand, which appears at 2.96 ppm. In the ^{13}C{^{1}H} NMR spectrum, the C$_\alpha$ and C$_\beta$ atoms of this ligand give rise to triplets at 308.5 ppm ($^{2}J_{C-P}$ = 12.8 Hz) and 117.0 ppm ($^{3}J_{C-P}$ = 3.8 Hz), respectively, whereas the resonances due to the metalated atoms of the acyl and imidazolylidene moieties appear at 233.7 and 180 ppm, also as triplets with C−P coupling constants of 6.8 and 7.6 Hz, respectively. The ^{31}P{^{1}H} NMR spectrum shows a singlet at −11.7 ppm for the equivalent phosphines. An acyl ν(CO) band at 1589 cm^{-1} in the IR spectrum is another characteristic feature of this compound.

Complex **4** is stable for several days in toluene under argon at room temperature. However, under a carbon monoxide atmosphere, it loses a phosphine ligand and evolves into Os{κ^2-*C*,*C*-[C(=CHPh)C(O)CH$_2$ImMe]}(CO)$_2$(P^{i}Pr$_3$) (**5**), as a result of the coordination of two carbon monoxide molecules and the 1,2-migratory insertion of the alkyne into the osmium−acyl bond. The replacement of the phosphine by carbonyl favors the migration.[35] This selective C−C bond formation is notable. In this context, it should be mentioned that the C−C coupling process on NHC ligands mainly takes place on the metalated carbon atom of the imidazolylidene moiety and involves intramolecular alkyl[36] or aryl[37] migration from palladium, alkyne insertion,[38] and external nucleophilic attack of a NHC group to η^1 metal allenyls[39] and α,β-unsaturated carbenes coordinated to chromium and tungsten.[40]

Complex **5** was isolated as a white solid in 40% yield and characterized by X-ray diffraction analysis. The structure proves the coupling, which gives rise to a six-membered metallacycle with a C(1)−Os−C(7) angle of 81.26(13)°: i.e., only about 3° higher than the C−Os−C angle of the five-membered ring of **4**. Figure 10 gives a view of the molecule. The coordination polyhedron around the osmium atom can be described as a distorted octahedron with the phosphine disposed trans to the imidazolylidene moiety (P−Os−C(1) = 171.15(9)°). The carbonyl ligands, which are disposed mutually cis (C(15)−Os−C(16) = 86.81(16)°), lie on the perpendicular plane. One of them is situated trans to the C(7) atom of the metallacycle (C(15)−Os−C(7) = 173.80(14)°), whereas the other is disposed trans to the chloride anion (C(16)−Os−Cl = 172.89(11)°). The Os−imidazolylidene bond length of 2.096(3) Å (Os−C(1)) is about 0.09 Å shorter than that in **4**. The osmium−alkenyl distance of 2.166(4) Å (Os−C(7)) is about 0.1 Å longer than the usual Os−C distance in osmium

DOI: 10.1021/acs.organomet.8b00110
Organometallics XXXX, XXX, XXX−XXX

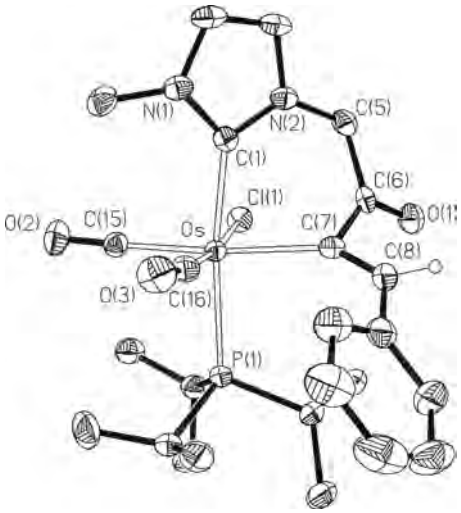

Figure 10. Molecular diagram of the cation of complex **5** (50% probability ellipsoids). Most hydrogen atoms are omitted for clarity. Selected bond lengths (Å) and angles (deg): Os−Cl(1) 2.4775(9), Os−P(1) 2.4591(9), Os−C(1) 2.096(3), Os−C(7) 2.166(4), Os−C(15) 1.918(3), Os−C(16) 1.851(4), C(6)−C(7) 1.500(5), C(7)−C(8) 1.349(5); Cl−Os−C(16) 172.89(11), P−Os−C(1) 171.15(9), C(7)−Os−C(15) 173.80(14), C(15)−Os−C(16) 86.81(16), Os−C(7)−C(8) 138.6(3).

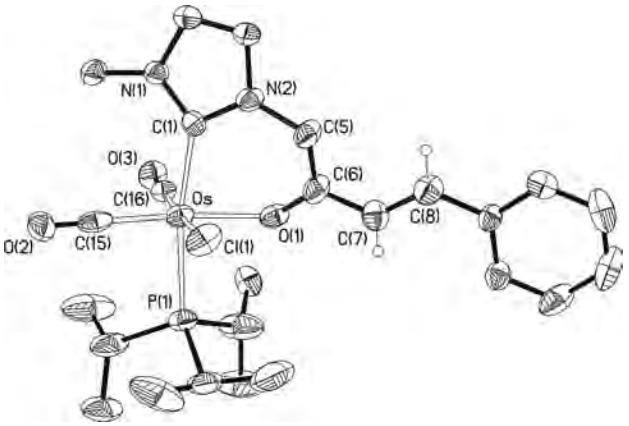

Figure 11. Molecular diagram of the cation of complex **6a** (50% probability ellipsoids). Most hydrogen atoms are omitted for clarity. Selected bond lengths (Å) and angles (deg): Os−Cl(1) 2.435(2), Os−P(1) 2.456(2), Os−O(1) 2.111(6), Os−C(1) 2.082(7), Os−C(15) 1.867(10), Os−C(16) 1.874(8), O(1)−C(6) 1.243(9), C(5)−C(6) 1.503(11), C(6)−C(7) 1.423(11), C(7)−C(8) 1.363(11); Cl(1)−Os−C(16) 173.8(2), P(1)−Os−C(1) 170.2(2), O(1)−Os−C(15) 173.7(3), O(1)−Os−C(1) 84.1(2), Os−O(1)−C(6) 129.1(5), O(1)−C(6)−C(7) 116.4(7), C(6)−C(7)−C(8) 123.2(8).

compounds with nonfunctionalized alkenyl groups.[41] However, it is the expected distance for a functionalized alkenyl ligand attached to osmium when the nucleophilicity transfer from C_α to C_β is not efficient.[42] In the $^{13}C\{^1H\}$ NMR spectrum, in benzene-d_6 at room temperature, the resonances corresponding to C(7) and C(1) atoms appear at 159.7 and 156.6 ppm as doublets with C−P coupling constants of 8.2 and 82.3 Hz, respectively, which are consistent with the position of the phosphine in the structure, cis to the first of them and trans to the second one. The phosphine gives rise to a singlet at 10.2 ppm, in the $^{31}P\{^1H\}$ NMR spectrum. In agreement with the cis dicarbonyl nature of the molecule, its IR spectrum shows two ν(CO) bands at 2002 and 1920 cm^{-1}.

Metal-mediated nucleophilic transfer from C_α to C_β does not occur effectively in **4**, in a manner consistent with the value of the Os−C(7) distance. Treatment of its dichloromethane solutions with $HBF_4{\cdot}OEt_2$ produces the protonation of C(7) instead of C(8). Nevertheless, the addition of the proton gives rise to a 1:0.3 mixture of the isomers $[OsCl(CO)_2\{\kappa^2\text{-}O,C\text{-}[O{=}C((E)\text{-}CH{-}CHPh)CH_2ImMe]\}(P^iPr_3)]BF_4$ (**6a**) and $[OsCl(CO)_2\{\kappa^2\text{-}O,C\text{-}[O{=}C((Z)\text{-}CH{-}CHPh)CH_2ImMe]\}(P^iPr_3)]BF_4$ (**6b**). The formation of this mixture suggests that the addition of the proton of the acid initially takes place at C_β, generating an intermediate (**G** in Scheme 5) with a C_α−C_β single bond. This allows an orientation change of the substituents, by rotation, which should lead to the isomeric mixture by a subsequent 1,2-hydrogen shift in any one of the rotamers.

Crystals suitable for X-ray diffraction analysis of salt **6a** was obtained from the mixture. Figure 11 gives a view of the cation. The structure proves the formation of the NHC-(α,β-unsaturated ketone) ligand, which acts as an O,C-chelate with an O(1)−Os−C(1) bite angle of 84.1(2)°. The coordination polyhedron around the osmium atom resembles that of **4** with the oxygen atom O(1) of the ketone in the position of the alkenyl C(7) atom and P−Os−C(1), C(15)−Os−O(1), and C(16)−Os−Cl angles of 170.2(2), 173.7(3), and 173.8(2)°, respectively. In agreement with the *E* stereochemistry of the C(7)−C(8) double bond, the resonances due to C(7)H and C(8)H (δ_H 8.50 and 7.14, respectively) display a H−H coupling constant of 16.1 Hz in the ^1H NMR spectrum. According to the trans disposition of the phosphine ligand and the imidazolylidene moiety, the $^{13}C\{^1H\}$ NMR spectrum contains a doublet with a C−P coupling constant of 84.0 Hz, at 158.7 ppm, due to C(1). The phosphine ligand gives rise to a singlet at 16.6 ppm in the $^{31}P\{^1H\}$ NMR spectrum. The analogous resonances of **6b** are observed at 7.64 and 6.68 ppm ($^3J_{H-H}$ = 11.8 Hz), 158.6 ppm ($^2J_{C-P}$ = 82.8 Hz), and 17.9 ppm in the respective ^1H, $^{13}C\{^1H\}$, and $^{31}P\{^1H\}$ NMR spectra.

CONCLUDING REMARKS

This study reveals new transformations of a NHC ligand coordinated to a transition metal, which contribute to destroy even further the myth of the robustness of this type of group to act as a spectator ligand in metal-promoted organic transformations, whereas some of these alterations prove that the imidazolylidene group can be used as a director to perform selective organic transformations. Furthermore, it demonstrates that the alterations in the NHC ligands can be not only thermally activated but also assisted by the organic substrate in a catalytic manner.

Internal alkynes promote the decarbonylation of the NHC-acyl ligand of complex $OsCl\{\kappa^2\text{-}C,C\text{-}[C(O)CH_3ImMe]\}(P^iPr_3)_2$. This hydrocarbon-catalyzed transformation involves a C−C cleavage, which gives rise to an unusual ring contraction from five membered to four membered. The resulting COsC metallacycle is unstable and undergoes a thermally activated 1,2-methylene shift from N to C, which is also uncommon, to afford a four-membered COsN heterometallacycle. The catalytic activity of the alkynes depends upon the electronic properties of the triple bond and the bulkiness of the substituents. The internal nature of the alkyne is determinant for the catalysis. In contrast to diphenylacetylene, 1-phenyl-1-propyne, 3-hexyne, or 2-butyne, phenylacetylene tautomerizes

DOI: 10.1021/acs.organomet.8b00110
Organometallics XXXX, XXX, XXX−XXX

in the metal coordination sphere to afford a stable vinylidene derivative, which experiences the coupling of the acyl moiety and the vinylidene ligand, under a carbon monoxide atmosphere, in a stoichiometric manner. The metal center does not provide an effective nucleophilicity transfer from C_α to C_β in the resulting alkenyl unit. As a consequence, the addition of acid gives rise to a novel NHC-(α,β-unsaturated ketone) ligand, which acts as a C,O-chelate.

In conclusion, the range of processes of degradation−transformation of spectator NHC ligands is not limited to stoichiometric σ-bond activation reactions on their substituents or C−C couplings involving the metalated carbon atom of the imidazolylidene moiety but covers a wide range of transformations, including hydrocarbon-catalyzed degradations of the substituents, a thermally activated 1,2-carbon shift from N to C, or stoichiometric C−C coupling of substituents with organic molecules present in the reaction media.

EXPERIMENTAL SECTION

All reactions were carried out with rigorous exclusion of air using Schlenk-tube techniques. Acetone, methanol, tetrahydrofuran, and 2-propanol were dried and distilled under argon. Other solvents were obtained oxygen and water free from an MBraun solvent purification apparatus. NMR spectra were recorded on a Varian Gemini 2000, a Bruker ARX 300 MHz, a Bruker Avance 300 MHz, or a Bruker Avance 400 MHz instrument. Chemical shifts (expressed in parts per million) are referenced to residual solvent peaks (^{1}H, ^{1}H{^{31}P}, ^{13}C{^{1}H}) or external standard (^{31}P{^{1}H} to 85% H_3PO_4 and ^{11}B to $BF_3{\cdot}OEt_2$). Coupling constants J and N ($N = J(PH) + J(P'H)$ for ^{1}H and $N = J(PC) + J(P'C)$ for ^{13}C{^{1}H}) are given in hertz. Attenuated total reflection infrared spectra (ATR-IR) of solid samples were run on a PerkinElmer Spectrum 100 FT-IR spectrometer. C, H, and N analyses were carried out in a PerkinElmer 2400 CHNS/O analyzer. High-resolution electrospray mass spectra (HRMS) were acquired using a MicroTOF-Q hybrid quadrupole time-of-flight spectrometer (Bruker Daltonics, Bremen, Germany). All reagents were purchased from commercial sources and used without further purification. OsCl{κ^2-*C,C*-[C(O)CH_2ImMe]}(P^iPr_3)$_2$ (**1**) was prepared according to the published method.[16]

Tranformation of Os{κ^2-*C,C*-[C(O)CH_2ImMe]}Cl(P^iPr_3)$_2$ (1) into Os{κ^2-*C,N*-[CH_2ImMe]}Cl(CO)(P^iPr_3)$_2$ (2) Mediated by Diphenylacetylene. A solution of **1** (0.100 g, 0.149 mmol) in toluene (5 mL) was treated with diphenylacetylene (0.107 g, 0.600 mmol). The mixture was stirred for 24 h at 100 °C, affording a brown solution, which was concentrated to dryness. The resulting solid was washed with methanol (2 × 2 mL), at approximately −70 °C, and dried in vacuo. Then, the solid was washed with pentane (4 × 2 mL) and dried in vacuo, obtaining a white solid. Yield: 0.020 g (20%). A crystal suitable for an X-ray diffraction study was obtained from slow diffusion of pentane in a concentrated solution of **2** in toluene. Anal. Calcd for $C_{24}H_{49}ClN_2OOsP_2$: C, 43.07; H, 7.38; N, 4.19. Found: C, 43.33; H, 7.27; N, 3.98. HRMS (electrospray, m/z): calcd for $C_{24}H_{49}N_2OOsP_2$ $[M - Cl]^+$ 635.2930, found 635.2970. IR (cm^{-1}): ν(C≡O) 1870 (s). ^{1}H NMR (300 MHz, CD_2Cl_2, 298 K): δ 6.97 (d, $^3J_{H-H}$ = 1.4, 1H, $CH_{imidazole}$), 6.43 (d, $^3J_{H-H}$ = 1.4, 1H, $CH_{imidazole}$), 3.38 (s, 3H, NCH_3), 2.66−2.51 (m, 6H, PCH), 2.27 (vt, $^3J_{H-P}$ = 3.0, 2H, CH_2), 1.26 (dvt, N = 12.6, $^3J_{H-H}$ = 6.9, 18H, PCH(CH_3)$_2$), 1.12 (dvt, N = 12.9, $^3J_{H-H}$ = 6.9, 18H, PCH(CH_3)$_2$). ^{13}C{^{1}H}-APT NMR plus HSQC and HMBC (75.5 MHz, CD_2Cl_2, 298 K): δ 188.3 (t, $^2J_{C-P}$ = 10.8, CO), 158.9 (s, NCN), 126.2 (s, $CH_{imidazole}$), 117.4 (s, $CH_{imidazole}$), 30.9 (s, NCH_3), 24.3 (vt, N = 22.9, PCH), 20.0 and 19.7 (both s, PCH(CH_3)$_2$), −31.5 (t, $^2J_{C-P}$ = 4.8, $OsCH_2$). ^{31}P{^{1}H} NMR (121.5 MHz, CD_2Cl_2, 298 K): δ 3.5 (s).

Characterization of Os{κ^2-*C,C*-[CH_2ImMe]}Cl(CO)(P^iPr_3)$_2$ (3). A solution of **1** (0.150 g, 0.224 mmol) in toluene (5 mL) was treated with diphenylacetylene (0.048 g, 0.269 mmol). The mixture was stirred for 1 h at 95 °C, affording a brown solution, which was concentrated to dryness. The resulting solid was washed with methanol (4 × 2 mL), at approximately −70 °C, and dried in vacuo. The resulting solid was washed with pentane (4 × 1 mL) to give a white solid, which was dried in vacuo. Yield: 0.031 g (20%). A crystal suitable for X-ray diffraction study was obtained from slow diffusion of pentane in a concentrated solution of **3** in dichloromethane. Anal. Calcd for $C_{24}H_{49}ClN_2OOsP_2$: C, 43.07; H, 7.38; N, 4.19. Found: C, 42.67; H, 7.07; N, 3.80. HRMS (electrospray, m/z): calcd for $C_{24}H_{49}N_2OOsP_2$ $[M - Cl]^+$ 635.2930, found 635.3018. IR (cm^{-1}): ν(CO) 1870 (s). ^{1}H NMR (300 MHz, C_6D_6, 298 K): δ 6.02 (d, $^3J_{H-H}$ = 1.8, 1H, $CH_{imidazole}$), 5.47 (d, $^3J_{H-H}$ = 1.8, 1H, $CH_{imidazole}$), 3.46 (vt, $^3J_{H-P}$ = 3.3, 2H, CH_2), 3.09 (s, 3H, NCH_3), 2.71−2.57 (m, 6H, PCH), 1.40 (dvt, N = 13.5, $^3J_{H-H}$ = 7.2, 18H, PCH(CH_3)$_2$), 1.03 (dvt, N = 12.3, $^3J_{H-H}$ = 6.9, 18H, PCH(CH_3)$_2$). ^{13}C{^{1}H}-APT NMR plus HSQC and HMBC (75.5 MHz, C_6D_6, 298 K): δ 191.3 (t, $^2J_{C-P}$ = 8.8, CO), 141.6 (t, $^2J_{C-P}$ = 6.9, NCN), 123.9 (s, $CH_{imidazole}$), 117.5 (s, $CH_{imidazole}$), 34.8 (s, NCH_3), 24.1 (vt, N = 24.0, PCH), 20.9 and 19.2 (both s, PCH(CH_3)$_2$), 17.3 (t, $^2J_{C-P}$ = 8.7, $OsCH_2$). ^{31}P{^{1}H} NMR (121.5 MHz, C_6D_6, 298 K): δ 2.1 (s).

Formation of a Mixture Enriched in Os{κ^2-*C,C*-[CH_2ImMe]}-Cl(CO)(P^iPr_3)$_2$ (3a). A solution of **1** (0.015 g, 0.022 mmol) in C_6D_6 (0.5 mL) was treated with diphenylacetylene (0.004 g, 0.022 mmol). The mixture was heated for 2 h at 75 °C, affording a brown solution which was a mixture of complexes **1**−**3** and **3a**. After one night at room temperature, crystals from **1** were obtained. The solution was filtered so that the resulting solution was more concentrated in **2**, **3**, and **3a**. Since signals from **2** and **3** were known, signals from **3a** were obtained by subtraction. ^{1}H NMR (400 MHz, C_6D_6, 298 K): δ 5.91 (d, $^3J_{H-H}$ = 1.6, 1H, $CH_{imidazole}$), 5.64 (d, $^3J_{H-H}$ = 1.6, 1H, $CH_{imidazole}$), 3.72 (vt, $^3J_{H-P}$ = 2.1, 2H, CH_2), 3.43 (s, 3H, NCH_3), 2.77−2.69 (m, 6 H, PCH), 1.28−1.10 (m, 36H, PCH(CH_3)$_2$). ^{13}C{^{1}H}-APT NMR plus HSQC and HMBC (100.6 MHz, C_6D_6, 298 K): δ 193.1 (t, $^2J_{C-P}$ = 12.1, CO), 155.2 (t, $^2J_{C-P}$ = 11.3, NCN), 120.0 (s, $CH_{imidazole}$), 119.0 (s, $CH_{imidazole}$), 37.9 (s, NCH_3), 24.3 (vt, N = 22.6, PCH), 19.9 and 19.6 (both s, PCH(CH_3)$_2$), −3.8 (t, $^2J_{C-P}$ = 5.3, $OsCH_2$). ^{31}P{^{1}H} NMR (162 MHz, C_6D_6, 298 K): δ 0.0 (s).

Formation of OsCl{κ^2-*C,C*-[C(O)CH_2ImMe]}(=C=CHPh)-(P^iPr_3)$_2$ (4). A solution of **1** (0.100 g, 0.149 mmol) in acetone (5 mL) was treated with phenylacetylene (18 μL, 0.163 mmol). The mixture was stirred at room temperature for 1 h, and the resulting solution was dried in vacuo. Subsequent addition of diethyl ether (3 mL) to the resulting residue, at approximately −70 °C, led to the formation of a pale pink solid, which was washed with further portions of diethyl ether (2 × 3 mL) and dried in vacuo. Yield: 0.076 g (66%). A crystal suitable for an X-ray diffraction study was obtained from a concentrated solution of **4** in acetone. Anal. Calcd for $C_{32}H_{55}ClN_2P_2OOs$: C, 49.82; H, 7.18; N, 3.63. Found: C, 49.45; H, 7.18; N, 3.96. HRMS (electrospray, m/z): calcd for $C_{32}H_{55}N_2P_2OOs$ $[M - Cl]^+$ 737.3400, found 737.3440. IR (cm^{-1}): ν(Os=C=C) 1614 (m); ν(C=O) 1589 (s). ^{1}H NMR (400 MHz, C_6D_6, 298 K): δ 7.53 (br, 2H, CH_{Ph}), 7.27 (dd, $^3J_{H-H}$ = 7.6, $^3J_{H-H}$ = 7.6, 2H, CH_{Ph}), 6.85 (t, $^3J_{H-H}$ = 7.6, 1H, CH_{Ph}), 6.10 (s, 1H, $CH_{imidazole}$), 5.97 (s, 1H, $CH_{imidazole}$), 3.99 (s, 3H, NCH_3), 3.43 (s, 2H, NCH_2), 2.96 (br, 1 H, *CH*Ph) 2.74−2.62 (m, 6H, PCH), 1.23 (dvt, $^3J_{H-H}$ = 6.4, N = 12.8, 18H, PCH(CH_3)$_2$), 1.18 (dvt, $^3J_{H-H}$ = 6.4, N = 12.8, 18H, PCH(CH_3)$_2$). ^{13}C{^{1}H}-APT NMR plus HSQC and HMBC (75.5 MHz, C_6D_6, 298 K): δ 308.6 (t, $^2J_{C-P}$ = 12.8, Os=*C*=C), 233.7 (t, $^2J_{C-P}$ = 6.8, C=O), 180.0 (t, $^2J_{C-P}$ = 7.6, *NC*N), 131.1 (t, $^4J_{C-P}$ = 2.3, C_{ipso}), 128.2 (s, CH_{Ph}), 126.7 (s, CH_{Ph}), 125.4 (s, $CH_{imidazole}$), 123.5 (s, CH_{Ph}), 117.0 (t, $^3J_{C-P}$ = 3.8, *C*HPh), 116.9 (s, $CH_{imidazole}$), 74.4 (s, CH_2), 37.1 (s, NCH_3), 26.1 (vt, N = 23.4, PCH), 20.3 and 20.0 (both s, PCH(CH_3)$_2$). ^{31}P{^{1}H} NMR (162.0 MHz, C_6D_6, 298 K): δ −11.7 (s).

Reaction of OsCl{κ^2-*C,C*-[C(O)CH_2ImMe]}(=C=CHPh)(P^iPr_3)$_2$ (4) with CO: Formation of Os{κ^2-*C,C*-[C(=CHPh)C(O)-CH_2ImMe]}(CO)$_2$(P^iPr_3) (5). A solution of **4** (0.090 g; 0.117 mmol) in toluene (5 mL) was stirred under a CO atmosphere (1 atm) for 3 days. The resulting solution was dried in vacuo, was washed first with pentane (2 × 2 mL) and dried in vacuo, and was then washed with MeOH (2 × 2 mL). A white solid was obtained. Yield: 0.030 g (39%). A crystal suitable for an X-ray diffraction study was obtained from slow

DOI: 10.1021/acs.organomet.8b00110
Organometallics XXXX, XXX, XXX−XXX

diffusion of pentane in a concentrated solution of **5** in toluene. Anal. Calcd for $C_{25}H_{34}ClN_2O_3OsP$: C, 45.00; H, 5.14; N, 4.20. Found: C, 44.79; H, 5.38; N, 3.95. HRMS (electrospray, *m/z*): calcd for $C_{25}H_{34}ClN_2NaO_3OsP$ $[M + Na]^+$ 691.1493, found 691.1505. IR (cm^{-1}): ν(CO) 2002 (s), 1920 (s), ν(C═O) 1162 (m). ^1H NMR (300 MHz, C_6D_6, 298 K): δ 8.18 (s, 1H, PhC*H*), 7.30 (d, $^3J_{H-H}$ = 7.2, 2H, CH_{Ph}), 7.16 (dd, $^3J_{H-H}$ = 7.2, $^3J_{H-H}$ = 7.2, 2H, CH_{Ph}), 7.03 (t, $^3J_{H-H}$ = 7.2, 1H, CH_{Ph}), 5.66 (s, 1H, $CH_{imidazole}$), 5.66 (s, 1H, $CH_{imidazole}$),5.46 (d, $^2J_{H-H}$ = 17.7, 1H, CH_2), 3.86 (d, $^2J_{H-H}$ = 17.7, 1H, CH_2), 3.21 (s, 3 H, NCH_3), 2.63−2.45 (m, 3H, PCH), 1.37 (dd, $^3J_{H-P}$ = 14.9, $^3J_{H-H}$ = 7.1, 9H, PCH(CH_3)$_2$), 0.74 (dd, $^3J_{H-P}$ = 12.2, $^3J_{H-H}$ = 7.1, 9H, PCH(CH_3)$_2$). $^{13}C\{^1H\}$−APT NMR plus HSQC and HMBC (75.5 MHz, C_6D_6, 298 K): δ 204.6 (s, C═O), 184.5 (d, $^2J_{C-P}$ = 6.9, CO), 180.2 (d, $^2J_{C-P}$ = 7.6, CO), 159.7 (d, $^2J_{C-P}$ = 8.2, C═CHPh), 156.6 (d, $^2J_{C-P}$ = 82.3, NCN), 143.1 (s, C_{ipso}), 140.0 (d, $^3J_{C-P}$ = 3.2, C═*C*HPh), 129.9 (s, Ph), 128.1 (s, Ph, overlapped with solvent signal), 126.5 (s, Ph), 121.7 (d, $^4J_{P-C}$ = 2.2, $CH_{imidazole}$), 121.6 (d, $^4J_{P-C}$ = 2.9, $CH_{imidazole}$), 59.7 (s, CH_2), 38.1 (s, NCH_3), 23.9 (d, $^1J_{C-P}$ = 24.3, PCH), 20.8 (s, PCH(CH_3)$_2$), 18.6 (d, $^2J_{C-P}$ = 3.4, PCH(CH_3)$_2$). $^{31}P\{^1H\}$ NMR (121.5 MHz, CD_2Cl_2, 298 K): δ 10.2 (s).

Protonation of Os{κ^2-*C*,*C*-[C(═CHPh)C(O)CH_2ImMe]}-$(CO)_2(P^iPr_3)$ (5): Formation of [OsCl(CO)$_2${κ^2-O,C-[O═C((*E*/*Z*)-CH−CHPh)CH_2ImMe]}(P^iPr_3)]BF_4 (6). A solution of **5** (0.050 g; 0.075 mmol) in dichloromethane (5 mL) was treated with HBF_4 for 5 min, resulting in a mixture of isomers **6a** and **6b** (*E*/*Z* ratio 0.7/1) that evolves to a thermodynamic ratio of **6a** and **6b** (*E*/*Z*) of 1/0.3 in 3 weeks. The resulting solution was dried in vacuo, washed with diethyl ether (2 × 2 mL) at approximately −70 °C, and dried in vacuo. A yellow solid was obtained. Yield: 0.045 g (80%). A crystal from the **6a** (*E*) isomer suitable for X-ray diffraction study was obtained from slow diffusion of pentane in a concentrated solution of the mixture in dichloromethane. Anal. Calcd for $C_{25}ClBH_{35}F_4N_2O_3OsP$: C, 39.77; H, 4.67; N, 3.71. Found: C, 39.43; H, 4.94; N, 3.47. HRMS (electrospray, *m/z*): calcd for $C_{25}H_{35}ClN_2O_3OsP$ $[M]^+$ 669.1673, found 669.1644. IR (cm^{-1}): ν(CO) 2032 (s), 1957 (s), ν(C═O) 1563 (m), $\nu(BF_4)$ 1055, 1033 (s).

(6a, E). ^1H NMR (300 MHz, CD_2Cl_2, 298 K): δ 8.50 (d, $^3J_{H-H}$ = 16.1 1H, C*H*═CHPh), 7.89−7.83 (m, 2H, CH_{Ph}), 7.69 (d, $^3J_{H-H}$ = 1.8, 1H, $CH_{imidazole}$), 7.65−7.57 (m, 1H, CH_{Ph}), 7.56−7.51 (m, 2H, CH_{Ph}) 7.20 (d, $^3J_{H-H}$ = 1.8, 1H, $CH_{imidazole}$), 7.14 (d, $^3J_{H-H}$ = 16.1, 1H, CH═C*H*Ph), 5.97 (AB spin system, $\Delta\nu$ = 85, $^2J_{AB}$ = 18.3, 2H, CH_2), 3.98 (s, 3H, NCH_3), 2.94−2.81 (m, 3H, PCH), 1.45 (dd, $^3J_{H-P}$ = 14.4, $^3J_{H-H}$ = 7.2, 9H, PCH(CH_3)$_2$), 1.42 (dd, $^3J_{H-P}$ = 13.8, $^3J_{H-H}$ = 7.2, 9H, PCH(CH_3)$_2$). $^{13}C\{^1H\}$-APT NMR plus HSQC and HMBC (75.5 MHz, CD_2Cl_2, 298 K): δ 204.8 (d, $^3J_{C-P}$ = 0.9, C═O), 178.4 (d, $^2J_{C-P}$ = 7.0, CO), 173.7 (d, $^2J_{C-P}$ = 7.0, CO), 158.7 (d, $^2J_{C-P}$ = 84.0, NCN), 158.2 (s, *C*H═CHPh), 135.0 (s, Ph), 133.5 (s, C_{ipso}), 131.5 (s, Ph), 130.1 (s, Ph), 124.6 (d, $^4J_{P-C}$ = 2.7, $CH_{imidazole}$), 124.5 (d, $^4J_{P-C}$ = 2.6, $CH_{imidazole}$), 123.2 (s, CH═*C*HPh), 54.6 (s, CH_2), 39.2 (s, NCH_3), 24.9 (d, $^1J_{C-P}$ = 25.1, PCH), 19.8 (s, PCH(CH_3)$_2$), 19.5 (d, $^2J_{C-P}$ = 1.8, PCH(CH_3)$_2$). $^{31}P\{^1H\}$ NMR (121.5 MHz, CD_2Cl_2, 298 K): δ 16.6 (s).

(6b, Z). ^1H NMR (300 MHz, CD_2Cl_2, 298 K): δ 7.67 (d, $^3J_{H-H}$ = 1.5, 1H, $CH_{imidazole}$), 7.65 (d, $^3J_{H-H}$ = 11.8 1H, C*H*═CHPh), 7.60−7.42 (m, 5H, CH_{Ph}), 7.21 (d, $^3J_{H-H}$ = 1.5, 1H, $CH_{imidazole}$), 6.68 (d, $^3J_{H-H}$ = 11.8, 1H, CH═C*H*Ph), 5.65 (AB spin system, $\Delta\nu$ = 137.82, $^2J_{AB}$ = 18.5, 2 H, CH_2), 3.96 (s, 3H, NCH_3), 2.83−2.68 (m, 1H, PCH), 2.52−2.36 (m, 2H, PCH), 1.33 (dd, $^3J_{H-P}$ = 12.6, $^3J_{H-H}$ = 7.2, 6H, PCH(CH_3)$_2$), 1.26 (dd, $^3J_{H-P}$ = 15.0, $^3J_{H-H}$ = 7.2, 6H, PCH(CH_3)$_2$), 1.16 (dd, $^3J_{H-P}$ = 12.9, $^3J_{H-H}$ = 7.8, 6H, PCH(CH_3)$_2$). $^{13}C\{^1H\}$ NMR plus HSQC and HMBC (75.5 MHz, CD_2Cl_2, 298 K) δ 208.1 (s, C═O), 178.0 (d, $^2J_{C-P}$ = 7.2, CO), 173.7 (d, $^2J_{C-P}$ = 6.8, CO), 158.6 (d, $^2J_{C-P}$ = 82.8, NCN), 155.3 (s, CH═CHPh), 134.8 (s, C_{ipso}), 132.6 (s, Ph), 130.3 (s, Ph), 129.9 (s, Ph), 125.0 (s, CH═*C*HPh), 124.8 (d, $^4J_{P-C}$ = 2.0, $CH_{imidazole}$), 124.6 (d, $^4J_{P-C}$ = 2.5, $CH_{imidazole}$), 58.6 (s, CH_2), 39.4 (s, NCH_3), 23.8 (d, $^1J_{C-P}$ = 25.2, PCH), 20.1 (s, PCH(CH_3)$_2$), 19.3 (d, $^2J_{C-P}$ = 2.8, PCH(CH_3)$_2$). $^{31}P\{^1H\}$ NMR (121.5 MHz, CD_2Cl_2, 298 K): δ 17.9 (s).

Structural Analysis of Complexes 2−5 and 6a. X-ray data were collected for the complexes on a Bruker Smart APEX CCD DUO diffractometer equipped with a fine focus, 2.4 kW sealed-tube source (Mo radiation, λ = 0.71073 Å). Data were collected over the complete sphere covering 0.3° in ω. Data were corrected for absorption by using a multiscan method applied with the SADABS program.[43] The structures were solved by Patterson or direct methods and refined by full-matrix least squares on F^2 with SHELXL97,[44] including isotropic and subsequently anisotropic displacement parameters. The hydrogen atoms were observed in the least-squares Fourier maps or calculated and refined freely or refined using a restricted riding model.

In **3** the crystal was found to be nonmerohedrally twinned. The orientation matrices for the two components were identified using the program Cell Now,[45] and the two components were integrated using Apex2. The twin matrix was found to be −1.003 0.012 0.488 −0.012 −0.995 0.492 0.004 0.002 0.998. The data were corrected for absorption using Twinabs,[46] and the structure was refined using hklf 5.

Crystal data for ***2:*** $C_{24}H_{49}ClN_2OOsP_2$, mol wt 669.24, colorless, irregular block (0.153 × 0.088 × 0.028 mm^3), monoclinic, space group $P2_1/n$, a =10.462(2) Å, b = 15.831(3) Å, c = 17.057(3) Å, β = 102.644(3)°, V = 2756.6(9) Å^3, Z = 4, Z' = 1, D_{calc} = 1.613 g cm^{-3}, $F(000)$ = 1352, T = 100(2) K, μ = 4.858 mm^{-1}; 30280 measured reflections (2θ = 3−58°, ω scans 0.3°), 7252 unique reflection (R_{int} = 0.0596); minimum/maximum transmission factors 0.717/0.862; final agreement factors R1 = 0.0333 (5544 observed reflections, $I > 2\sigma(I)$) and wR2 = 0.0693; data/restraints/parameters 7252/9/291; GOF = 1.000; largest peak and hole 1.559 (close to osmium atom) and −1.079 e Å^{-3}.

Crystal data for ***3:*** $C_{24}H_{49}ClN_2OOsP_2$, CH_2Cl_2, mol wt 754.16, colorless, irregular block (0.22 × 0.16 × 0.14 mm^3), triclinic, space group $P\bar{1}$, a = 13.7819(15) Å, b = 14.9756(16) Å, c = 17.6750(19) Å, α = 73.1980(10)°, β = 71.821(2)°, γ = 67.4180(10)°, V = 3140.0(6) Å^3, Z = 4, Z' = 2, D_{calc} = 1.595 g cm^{-3}, $F(000)$ = 1520, T = 100(2) K, μ = 4.439 mm^{-1}; 15801 measured reflections (2θ = 3−58°, ω scans 0.3°), 15801 unique reflections; minimum/maximum transmission factors 0.627/0.745; final agreement factors R1 = 0.0339 (12698 observed reflections, $I > 2\sigma(I)$) and wR2 = 0.0923; data/restraints/parameters 15801/0/640; GOF = 1.064; largest peak and hole 3.188 (close to osmium atoms) and −1.962 e Å^{-3}.

Crystal data for ***4:*** $C_{32}H_{55}ClN_2OOsP_2$, mol wt 771.37, orange, irregular block (0.122 × 0.103 × 0.052 mm^3), monoclinic, space group Cc, a = 10.9699(6) Å, b = 20.2848(11) Å, c = 15.1982(8) Å, β = 98.1480(10)°, V = 3347.8(3) Å^3, Z = 4, Z' = 1, D_{calc} = 1.530 g cm^{-3}, $F(000)$ = 1568, T = 100(2) K, μ = 4.011 mm^{-1}; 20187 measured reflections (2θ = 3−58°, ω scans 0.3°), 7781 unique reflections (R_{int} = 0.0348); minimum/maximum transmission factors 0.712/0.862; final agreement factors R1 = 0.0344 (7296 observed reflections, $I > 2\sigma(I)$) and wR2 = 0.0829; Flack parameter −0.026(10); data/restraints/parameters 7781/2/369; GOF = 1.006; largest peak and hole 2.599 (close to osmium atoms) and −0.998 e Å^{-3}.

Crystal data for ***5:*** $C_{25}H_{34}ClN_2O_3OsP$, mol wt 667.16, colorless, irregular block (0.109 × 0.060 × 0.060 mm^3), monoclinic, space group $P2_1/c$, a = 16.931(3) Å, b = 9.5542(14) Å, c = 16.206(2) Å, β = 94.117(2)°, V = 2614.8(7) Å^3, Z = 4, Z' = 1, D_{calc} = 1.695 g cm^{-3}, $F(000)$ = 1320, T = 150(2) K, μ = 5.069 mm^{-1}; 29036 measured reflections (2θ = 3−58°, ω scans 0.3°), 6320 unique reflections (R_{int} = 0.0411); minimum/maximum transmission factors 0.697/0.862; final agreement factors R1 = 0.0285 (5528 observed reflections, $I > 2\sigma(I)$) and wR2 = 0.0599; data/restraints/parameters 6320/0/308; GOF = 1.106; largest peak and hole 1.289 (close to osmium atoms) and −0.793 e Å^{-3}.

Crystal data for ***6a:*** $C_{25}H_{35}ClN_2O_3OsP$, BF_4, mol wt 754.98, colorless, irregular block (0.203 × 0.075 × 0.066 mm^3), monoclinic, space group $P2_1/c$, a = 12.8749(13) Å, b = 14.5959(15) Å, c = 16.4490(17) Å, β = 111.0240(10)°, V = 2885.3(5) Å^3, Z = 4, Z' = 1, D_{calc} = 1.738 g cm^{-3}, $F(000)$ = 1488, T = 100(2) K, μ = 4.623 mm^{-1}. 24584 measured reflections (2θ = 3−58°, ω scans 0.3°), 6827 unique reflections (R_{int} = 0.0552); minimum/maximum transmission factors 0.632/0.862; final agreement factors R1 = 0.0545 (5047 observed reflections, $I > 2\sigma(I)$) and wR2 = 0.1323; data/restraints/parameters

DOI: 10.1021/acs.organomet.8b00110
Organometallics XXXX, XXX, XXX−XXX

6827/0/350; GOF = 3.677; largest peak and hole −2.828 (close to osmium atoms) and −0.793 e $Å^{-3}$.

■ ASSOCIATED CONTENT

Supporting Information

The Supporting Information is available free of charge on the ACS Publications website at DOI: 10.1021/acs.organomet.8b00110.

^{1}H, $^{31}P\{^{1}H\}$ and $^{13}C\{^{1}H\}$ spectra of **2**−**5** and mixtures enriched in **3a** and **6a**,**b**, computational details, full reaction profile, and energies of calculated complexes (PDF)

Theoretical complex coordinates (XYZ)

Accession Codes

CCDC 1542128−1542129 and 1824793−1824795 contain the supplementary crystallographic data for this paper. These data can be obtained free of charge via www.ccdc.cam.ac.uk/data_request/cif, or by emailing data_request@ccdc.cam.ac.uk, or by contacting The Cambridge Crystallographic Data Centre, 12 Union Road, Cambridge CB2 1EZ, UK; fax: +44 1223 336033.

■ AUTHOR INFORMATION

Corresponding Author

*E-mail for M.A.E.: maester@unizar.es.

ORCID

Miguel A. Esteruelas: 0000-0002-4829-7590

M. Pilar Gay: 0000-0001-8056-1083

Enrique Oñate: 0000-0003-2094-719X

Notes

The authors declare no competing financial interest.

■ ACKNOWLEDGMENTS

Financial support from the MINECO of Spain (Project CTQ2017-82935-P), Gobierno de Aragón (E06_17R), FEDER, and the European Social Fund is acknowledged. M.P.G. thanks the Spanish MINECO for her FPI fellowship.

■ REFERENCES

(1) (a) Hahn, F. E.; Jahnke, M. C. Heterocyclic Carbenes: Synthesis and Coordination Chemistry. *Angew. Chem., Int. Ed.* **2008**, *47*, 3122−3172. (b) de Frémont, P.; Marion, N.; Nolan, S. P. Carbenes: Synthesis, Properties, and Organometallic Chemistry. *Coord. Chem. Rev.* **2009**, *253*, 862−892. (c) Hindi, K. M.; Panzner, M. J.; Tessier, C. A.; Cannon, C. L.; Youngs, W. J. The Medicinal Applications of Imidazolium Carbene-Metal Complexes. *Chem. Rev.* **2009**, *109*, 3859−3884. (d) Schuster, O.; Yang, L.; Raubenheimer, H. G.; Albrecht, M. Beyond Conventional N-Heterocyclic Carbenes: Abnormal, Remote, and Other Classes of NHC Ligands with Reduced Heteroatom Stabilization. *Chem. Rev.* **2009**, *109*, 3445−3478. (e) Poyatos, M.; Mata, J. A.; Peris, E. Complexes with Poly(N-Heterocyclic Carbene) Ligands: Structural Features and Catalytic Applications. *Chem. Rev.* **2009**, *109*, 3677−3707. (f) Hopkinson, M. N.; Richter, C.; Schedler, M.; Glorius, F. An overview of N-Heterocyclic Carbenes. *Nature* **2014**, *510*, 485−496. (g) Visbal, R.; Gimeno, C. N-Heterocyclic Carbene Metal Complexes: Photoluminescence and Applications. *Chem. Soc. Rev.* **2014**, *43*, 3551−3574. (h) Zhong, R.; Lindhorst, A. C.; Groche, F. J.; Kühn, F. E. Immobilization of N-Heterocyclic Carbene Compounds: A Synthetic Perspective. *Chem. Rev.* **2017**, *117*, 1970−2058.

(2) (a) Kantchev, E. A.; O'Brien, C. J.; Organ, M. G. Palladium Complexes of N-Heterocyclic Carbenes as Catalysts for Cross-Coupling Reactions—A Synthetic Chemist's Perspective. *Angew. Chem., Int. Ed.* **2007**, *46*, 2768−2813. (b) Marion, N.; Nolan, S. P. Well-Defined N-Heterocyclic Carbenes-Palladium(II) Precatalysts for Cross- Coupling Reactions. *Acc. Chem. Res.* **2008**, *41*, 1440−1449. (c) Díez-González, S.; Marion, N.; Nolan, S. P. N-Heterocyclic Carbenes in Late Transition Metal Catalysis. *Chem. Rev.* **2009**, *109*, 3612−3676. (d) Ramon, R. S.; Nolan, S. P. In *Applied Homogeneous Catalysis with Organometallic Compounds: A Comprehensive Handbook in Four Volumes*, 3rd ed.; Cornils, B., Herrmann, W. A., Beller, M., Paciello, R., Eds.; Wiley: Hoboken, NJ, 2017; Chapter 11.1, pp 809−828.

(3) (a) Crudden, C. M.; Allen, D. P. Stability and Reactivity of N-Heterocyclic Carbene Complexes. *Coord. Chem. Rev.* **2004**, *248*, 2247−2273. (b) Esteruelas, M. A.; López, A. M.; Oliván, M. Polyhydrides of Platinum Group Metals: Nonclassical Interactions and σ-Bond Activation Reactions. *Chem. Rev.* **2016**, *116*, 8770−8847.

(4) See for example: (a) Cabeza, J. A.; del Río, I.; Miguel, D.; Sánchez-Vega, M. G. Easy Activation of two C−H Conds of an N-heterocyclic Carbene N-methyl Group. *Chem. Commun.* **2005**, 3956−3958. (b) Cabeza, J. A.; del Río, I.; Miguel, D.; Sánchez-Vega, M. G. From an N-Methyl N-Heterocyclic Carbene to Carbyne and Carbide Ligands via Multiple C-H and C-N Bond Activations. *Angew. Chem., Int. Ed.* **2008**, *47*, 1920−1922. (c) Albrecht, M. Cyclometalation Using d-Block Transition Metals: Fundamental Aspects and Recent Trends. *Chem. Rev.* **2010**, *110*, 576−623. (d) Alabau, R. G.; Eguillor, B.; Esler, J.; Esteruelas, M. A.; Oliván, M.; Oñate, E.; Tsai, J.-Y.; Xia, C. CCC−Pincer−NHC Osmium Complexes: New Types of Blue-Green Emissive Neutral Compounds for Organic Light-Emitting Devices (OLEDs). *Organometallics* **2014**, *33*, 5582−5596. (e) Bolaño, T.; Esteruelas, M. A.; Fernández, I.; Oñate, E.; Palacios, A.; Tsai, J.-Y.; Xia, C. Osmium(II)−Bis(dihydrogen) Complexes Containing Car-yl,CNHC−Chelate Ligands: Preparation, Bonding Situation, and Acidity. *Organometallics* **2015**, *34*, 778−789. (f) Luy, J.-N.; Hauser, S. A.; Chaplin, A. B.; Tonner, R. Rhodium(I) and Iridium(I) Complexes of the Conformationally Rigid $IBioxMe_4$ Ligand: Computational and Experimental Studies of Unusually Tilted NHC Coordination Geometries. *Organometallics* **2015**, *34*, 5099−5112. (g) Eguillor, B.; Esteruelas, M. A.; Lezáun, V.; Oliván, M.; Oñate, E.; Tsai, J.-Y.; Xia, C. A Capped Octahedral MHC_6 Compound of a Platinum Group Metal. *Chem. - Eur. J.* **2016**, *22*, 9106−9110. (h) Yan, J.; Han, Z.; Zhang, D.; Liu, C. Theoretical Study of the Mechanism of two Successive N-Methylene C−H Bond Activations on a Phosphine-tethered N-Heterocyclic Carbene on a Triruthenium Carbonyl Cluster. *RSC Adv.* **2016**, *6*, 99625−99630. (i) Esteruelas, M. A.; Oñate, E.; Palacios, A.; Tsai, J.-Y.; Xia, C. Preparation of Capped Octahedral $OsHC_6$ Complexes by Sequential Carbon-Directed C−H Bond Activation Reactions. *Organometallics* **2016**, *35*, 2532−2542. (j) Alabau, R. G.; Esteruelas, M. A.; Oliván, M.; Oñate, E.; Palacios, A. U.; Tsai, J.-Y.; Xia, C. Osmium(II) Complexes Containing a Dianionic CCCC-Donor Tetradentate Ligand. *Organometallics* **2016**, *35*, 3981−3995. (k) Wenz, K. M.; Liu, P.; Houk, K. N. Intramolecular C−H Activation Reactions of Ru(NHC) Complexes Combined with H_2 Transfer to Alkenes: A Theoretical Elucidation of Mechanisms and Effects of Ligands on Reactivities. *Organometallics* **2017**, *36*, 3613−3623. (l) Esteruelas, M. A.; López, A. M.; Oñate, E.; San-Torcuato, A.; Tsai, J.-Y.; Xia, C. Formation of Dinuclear Iridium Complexes by NHC-Supported C−H Bond Activation. *Organometallics* **2017**, *36*, 699−707.

(5) See for example: (a) Jazzar, R. F. R.; Macgregor, S. A.; Mahon, M. F.; Richards, S. P.; Whittlesey, M. K. C-C and C-H Bond Activation Reactions in N-Heterocyclic Carbene Complexes of Ruthenium. *J. Am. Chem. Soc.* **2002**, *124*, 4944−4945. (b) Bolaño, T.; Buil, M. L.; Esteruelas, M. A.; Izquierdo, S.; Lalrempuia, R.; Oliván, M.; Oñate, E. C-C Bond Activation of the NHC Ligand of an Osmium-Amido Complex. *Organometallics* **2010**, *29*, 4517−4523. (c) Nugent, J. W.; Espinosa Martínez, G.; Gray, D. L.; Fout, A. R. Synthesis and Characterization of Bidentate NHC-CAryl Nickel(II) Complexes: Isocyanide Insertion To Form NHC-η^2-iminoacyl Complexes. *Organometallics* **2017**, *36*, 2987−2995.

(6) See for example: (a) Häller, L. J. L.; Page, M. J.; Erhardt, S.; Macgregor, S. A.; Mahon, M. F.; Naser, M. A.; Vélez, A.; Whittlesey,

DOI: 10.1021/acs.organomet.8b00110
Organometallics XXXX, XXX, XXX−XXX

M. K. Experimental and Computational Investigation of C-N Bond Activation in Ruthenium N-Heterocyclic Carbene Complexes. *J. Am. Chem. Soc.* **2010**, *132*, 18408−18416. (b) Xiang, L.; Xiao, J.; Deng, L. Synthesis, Structure, and Reactivity of Organo-Iron(II) Complexes with N-Heterocyclic Carbene Ligation. *Organometallics* **2011**, *30*, 2018−2015. (c) Day, B. M.; Pugh, T.; Hendriks, D.; Guerra, C. F.; Evans, D. J.; Bickelhaupt, F. M.; Layfield, R. A. Normal-to-Abnormal Rearrangement and NHC Activation in Three-Coordinate Iron(II) Carbene Complexes. *J. Am. Chem. Soc.* **2013**, *135*, 13338−13341. (d) Zhong, W.; Fei, Z.; Scopelliti, R.; Dyson, P. J. Alcohol-Induced C-N Bond Cleavage of Cyclometalated N-Heterocyclic Carbene Ligands with a Methylene-Linked Pendant Imidazolium Ring. *Chem. - Eur. J.* **2016**, *22*, 12138−12144.

(7) (a) Burling, S.; Paine, B. M.; Nama, D.; Brown, V. S.; Mahon, M. F.; Prior, T. J.; Pregosin, P. S.; Whittlesey, M. K.; Williams, J. M. J. C-H Activation Reactions of Ruthenium N-Heterocyclic Carbene Complexes: Application in a Catalytic Tandem Reaction Involving C-C Bond Formation from Alcohols. *J. Am. Chem. Soc.* **2007**, *129*, 1987−1995. (b) Vieille-Petit, L.; Luan, X.; Gatti, M.; Blumentritt, S.; Linden, A.; Clavier, H.; Nolan, S. P.; Dorta, R. Improving Grubbs' II type ruthenium catalysts by appropriately modifying the N-heterocyclic carbene ligand. *Chem. Commun.* **2009**, 3783−3785. (c) Choi, G.; Tsurugi, H.; Mashima, K. Hemilabile N-Xylyl-N′-methylperimidine Carbene Iridium Complexes as Catalysts for C−H Activation and Dehydrogenative Silylation: Dual Role of N-Xylyl Moiety for ortho-C−H Bond Activation and Reductive Bond Cleavage. *J. Am. Chem. Soc.* **2013**, *135*, 13149−13161. (d) Mo, Z.; Deng, L. Posts-Functionalization: A Useful Method for the Synthesis of Donor- Functionalized N-Heterocyclic Carbene−Transition-Metal Catalysts. *Synlett* **2014**, *25*, 1045−1049. (e) Paul, D.; Beiring, B.; Plois, M.; Ortega, N.; Kock, S.; Schlüns, D.; Neugebauer, J.; Wolf, R.; Glorius, F. A Cyclometalated Ruthenium-NHC Precatalyst for the Asymmetric Hydrogenation of (Hetero)arenes and Its Activation Pathway. *Organometallics* **2016**, *35*, 3641−3646. (f) Fizia, A.; Gaffga, M.; Lang, J.; Sun, J.; Niedner-Schatteburg, G.; Thiel, W. R. Cyclopalladation in the Periphery of a NHC Ligand as the Crucial Step in the Synthesis of Highly Active Suzuki−Miyaura Cross-Coupling Catalysts. *Chem. - Eur. J.* **2017**, *23*, 14563−14575.

(8) (a) Trnka, T. M.; Morgan, J. P.; Sanford, M. S.; Wilhelm, M. S.; Choi, T.-L.; Ding, S.; Day, M. W.; Grubbs, R. G. Synthesis and Activity of Ruthenium Alkylidene Complexes Coordinated with Phosphine and N-Heterocyclic Carbene Ligands. *J. Am. Chem. Soc.* **2003**, *125*, 2546−2558. (b) Hong, S. H.; Wenzel, A. G.; Salguero, T. T.; Day, M. W.; Grubbs, R. H. Decomposition of Ruthenium Olefin Metathesis Catalysts. *J. Am. Chem. Soc.* **2007**, *129*, 7961−7968. (c) Leitao, E. M.; Dubberley, S. R.; Piers, W. E.; Wu, Q.; McDonald, R. Thermal Decomposition Modes for Four-Coordinate Ruthenium Phosphonium Alkylidene Olefin Metathesis Catalysts. *Chem. - Eur. J.* **2008**, *14*, 11565−11572. (d) McClennan, W. L.; Rufh, S. A.; Lummiss, J. A. M.; Fogg, D. E. A General Decomposition Pathway for Phosphine-Stabilized Metathesis Catalysts: Lewis Donors Accelerate Methylidene Abstraction. *J. Am. Chem. Soc.* **2016**, *138*, 14668−14677. (e) Bailey, G. A.; Lummiss, J. A. M.; Foscato, M.; Occhipinti, G.; McDonald, R.; Jensen, V. R.; Fogg, D. E. Decomposition of Olefin Metathesis Catalysts by Brønsted Base: Metallacyclobutane Deprotonation as a Primary Deactivating Event. *J. Am. Chem. Soc.* **2017**, *139*, 16446−16449.

(9) (a) Liddle, S. T.; Edworthy, I. S.; Arnold, P. L. Anionic Tethered N-Heterocyclic Carbene Chemistry. *Chem. Soc. Rev.* **2007**, *36*, 1732−1744. (b) Pape, F.; Teichert, J. F. Dealing at Arm's Length: Catalysis with N-Heterocyclic Carbene Ligands Bearing Anionic Tethers. *Eur. J. Org. Chem.* **2017**, *2017*, 4206−4229.

(10) (a) Albrecht, M.; Miecznikowski, J. R.; Samuel, A.; Faller, J. W.; Crabtree, R. H. Chelated Iridium(III) Bis-carbene Complexes as Air-Stable Catalysts for Transfer Hydrogenation. *Organometallics* **2002**, *21*, 3596−3604. (b) Mata, J. A.; Chianese, A. R.; Miecznkowski, J. R.; Poyatos, M.; Peris, E.; Faller, J. W.; Crabtree, R. H. Reactivity Differences in the Syntheses of Chelating N-Heterocyclic Carbene Complexes of Rhodium Are Ascribed to Ligand Anisotropy. *Organometallics* **2004**, *23*, 1253−1263. (c) Leung, C. H.; Incarvito, C. D.; Crabtree, R. H. Interplay of Linker, N-Substituent, and Counterion Effects in the Formation and Geometrical Distortion of N-Heterocyclic Biscarbene Complexes of Rhodium(I). *Organometallics* **2006**, *25*, 6099−6107. (d) Wang, X.; Liu, S.; Weng, L.-H.; Jin, G.-X. Preparation and Structure of Mono- and Binuclear Half-Sandwich Iridium, Ruthenium, and Rhodium Carbene Complexes Containing 1,2-Dichalcogenolao 1,2-Dicarba-closo-Dodecaboranes. *Chem. - Eur. J.* **2007**, *13*, 188−195. (e) Zamora, M. T.; Ferguson, M. J.; McDonald, R.; Cowie, M. N-Heterocyclic Carbenes. *Dalton Trans.* **2009**, 7269−7287. (f) Riederer, S. K. U.; Gigler, P.; Högerl, M. P.; Herdtweck, E.; Bechlars, B.; Hermann, W. A.; Kühn, F. E. Impact of Ligand Modification on Structures and Catalytic Activities of Chelating Bis-Carbene Rhodium(I) Complexes. *Organometallics* **2010**, *29*, 5681−5692. (g) Graeupner, J.; Hintermair, U.; Huang, D. L.; Thomsen, J. M.; Takase, M.; Campos, J.; Hashmi, S. M.; Elimelech, M.; Brudving, G. W.; Crabtree, R. H. Probing the Viability of Oxo-Coupling Pathways in Iridium-Catalyzed Oxygen Evolution. *Organometallics* **2013**, *32*, 5384−5390. (h) Schick, S.; Pape, T.; Hahn, F. E. Coordination Chemistry of Bidentate Bis(NHC) Ligands with Two Different NHC Donors. *Organometallics* **2014**, *33*, 4035−4041.

(11) (a) Bierenstiel, M.; Cross, E. D. Sulfur-functionalized N-heterocyclic carbenes and their transition metal complexes. *Coord. Chem. Rev.* **2011**, *255*, 574−590. (b) Fliedel, C.; Braunstein, P. Recent Advances in S-Functionalized N-Heterocyclic Carbene Ligands: From the Synthesis of Azolium Salts and Metal Complexes to Applications. *J. Organomet. Chem.* **2014**, *751*, 286−300.

(12) Hameury, S.; de Frémont, P.; Braunstein, P. Metal Complexes with Oxygen-Functionalized NHC Ligands: Synthesis and Applications. *Chem. Soc. Rev.* **2017**, *46*, 632−733.

(13) (a) Gründemann, S.; Kovacevic, A.; Albrecht, M.; Faller, J. W.; Crabtree, R. H. Abnormal Binding in a Carbene Complex Formed from an Imidazolium Salt and a Metal Hydride Complex. *Chem. Commun.* **2001**, 2274−2275. (b) Kovacevic, A.; Gründemann, S.; Miecznikowski, J. R.; Clot, E.; Eisenstein, O.; Crabtree, R. H. Counter-ion Effects Switch Ligand Binding from C-2 to C-5 in Kinetic Carbenes Formed from an Imidazolium Salt and $IrH_5(PPh_3)_2$. *Chem. Commun.* **2002**, 2580−2581. (c) Gründemann, S.; Kovacevic, A.; Albrecht, M.; Faller, J. W.; Crabtree, R. H. Abnormal Ligand Binding and Reversible Ring Hydrogenation in the Reaction of Imidazolium Salts with $IrH_5(PPh_3)_2$. *J. Am. Chem. Soc.* **2002**, *124*, 10473−10481. (d) Crabtree, R. H. Carbenes. Pincers, Chelates, and Abnormal Binding Modes. *Pure Appl. Chem.* **2003**, *75*, 435−443. (e) Appelhans, L. N.; Zuccaccia, D.; Kovacevic, A.; Chianese, A. R.; Miecznikowski, J. R.; Macchioni, A.; Clot, E.; Eisenstein, O.; Crabtree, R. H. An Anion-Dependent Switch in Selectivity Results from a Change of C-H Activation Mechanism in the Reaction of an Imidazolium Salt with $IrH_5(PPh_3)_2$. *J. Am. Chem. Soc.* **2005**, *127*, 16299−16311. (f) Baya, M.; Eguillor, B.; Esteruelas, M. A.; Oliván, M.; Oñate, E. Influence of the Anion of the Salt Used on the Coordination Mode of an N-Heterocyclic Carbene Ligand to Osmium. *Organometallics* **2007**, *26*, 6556−6563. (g) Cross, W. B.; Daly, C. G.; Boutadla, Y.; Singh, K. Variable Coordination of Amine Functionalised N-Heterocyclic Carbene Ligands to Ru, Rh and Ir: C−H and N−H Activation and Catalytic Transfer Hydrogenation. *Dalton Trans.* **2011**, *40*, 9722−9730.

(14) Peris, E. Smart N-Heterocyclic Carbene Ligands in Catalysis. *Chem. Rev.* **2017**, DOI: 10.1021/acs.chemrev.6b00695.

(15) Aouat, Y.; Marom, G.; Avnir, D. Eur. J. Corrosion-Resistant Hybrid Nanoparticles of Polydimethylsiloxane@Fe Obtained by Thermolysis of $Fe(CO)_5$. *Eur. J. Inorg. Chem.* **2016**, *2016*, 1488−1496.

(16) Bolaño, T.; Esteruelas, M. A.; Gay, M. G.; Oñate, E.; Pastor, I. M.; Yus, M. An Acyl-NHC Osmium Cooperative System: Coordination of Small Molecules and Heterolytic B−H and O−H Bond Activation. *Organometallics* **2015**, *34*, 3902−3908.

(17) (a) Esteruelas, M. A.; López, A. M. In *Recent Advances in Hydride Chemistry*; Peruzzini, M., Poly, R.; Eds.; Elsevier: Amsterdam, 2001; Chapter 7, pp 189−248. (b) Esteruelas, M. A.; López, A. M. C-C Coupling and C-H Bond Activation Reactions of Cyclopentadienyl-

DOI: 10.1021/acs.organomet.8b00110
Organometallics XXXX, XXX, XXX−XXX

Osmium Compounds: The Rich and Varied Chemistry of Os(η^5-C_5H_5)Cl(P^iPr_3)$_2$ and Its Major Derivatives. *Organometallics* **2005**, *24*, 3584−3613. (c) Esteruelas, M. A.; López, A. M.; Oliván, M. Osmium−carbon Double Bonds: Formation and Reactions. *Coord. Chem. Rev.* **2007**, *251*, 795−840. (d) Bolaño, T.; Esteruelas, M. A.; Oñate, E. Osmium-carbon Multiple Bonds: Reduction and C-C Coupling Reactions. *J. Organomet. Chem.* **2011**, *696*, 3911−3923.

(18) (a) Satoh, T.; Miura, M. Oxidative Coupling of Aromatic Substrates with Alkynes and Alkenes under Rhodium Catalysis. *Chem. - Eur. J.* **2010**, *16*, 11212−11222. (b) Xiao, J.; Li, X. Gold α-Oxo Carbenoids in Catalysis: Catalytic Oxygen-Atom Transfer to Alkynes. *Angew. Chem., Int. Ed.* **2011**, *50*, 7226−7236. (c) Haydl, A. M.; Breit, B.; Liang, T.; Krische, M. Alkynes as Electrophilic or Nucleophilic Allylmetal Precursors in Transition-Metal Catalysis. *Angew. Chem., Int. Ed.* **2017**, *56*, 11312−11325. (d) Esteruelas, M. A., Oliván, M. In *Applied Homogeneous Catalysis with Organometallic Compounds: A Comprehensive Handbook in Four Volumes*, 3rd ed.; Cornils, B., Herrmann, W. A., Beller, M., Paciello, R., Eds.; Wiley: Hoboken, NJ, 2017; Chapter 23, pp 1307−1331.

(19) (a) Bellachioma, G.; Cardaci, G.; Macchioni, A.; Zanazzi, P. Oxidative Addition of Methyl Iodide to Monosubstituted and Disubstituted Derivatives of Osmium Pentacarbonyl. *Inorg. Chem.* **1993**, *32*, 547−553. (b) Esteruelas, M. A.; Carcía-Yebra, C.; Oliván, M.; Oñate, E.; Valencia, M. Osmium-Catalyzed Allylic Alkylation. *Organometallics* **2008**, *27*, 4892−4902. (c) Baya, M.; Esteruelas, M. A.; Oñate, E. Efficient Concatenation of C═C Reduction, C-H Bond Activation, and C-C and C-N Coupling Reactions on Osmium: Assembly of Two Allylamines and an Allene. *Organometallics* **2010**, *29*, 6298−6307. (d) Esteruelas, M. A.; López, A. M.; López, F.; Mascareñas, J. L.; Mozo, S.; Oñate, E.; Saya, L. Osmium Models of Intermediates Involved in Catalytic Reactions of Alkylidenecyclopropanes. *Organometallics* **2013**, *32*, 4851−4861.

(20) (a) Eguillor, B.; Esteruelas, M. A.; García-Raboso, J.; Oliván, M.; Oñate, E.; Pastor, I. M.; Peñafiel, I.; Yus, M. Osmium NHC Complexes from Alcohol-Functionalized Imidazoles and Imidazolium Salts. *Organometallics* **2011**, *30*, 1658−1667. (b) Buil, M. L.; Cardo, J. J. F.; Esteruelas, M. A.; Fernández, I.; Oñate, E. Hydroboration and Hydrogenation of an Osmium−Carbon Triple Bond: Osmium Chemistry of a Bis-σ-Borane. *Organometallics* **2015**, *34*, 547−550. (c) Buil, M. L.; Cardo, J. J. F.; Esteruelas, M. A.; Oñate, E. Dehydrogenative Addition of Aldehydes to a Mixed NHC-Osmium-Phosphine Hydroxide Complex: Formation of Carboxylate Derivatives. *Organometallics* **2016**, *35*, 2171−2173. (d) Buil, M. L.; Cardo, J. J. F.; Esteruelas, M. A.; Oñate, E. Square-Planar Alkylidyne−Osmium and Five-Coordinate Alkylidene−Osmium Complexes: Controlling the Transformation from Hydride-Alkylidyne to Alkylidene. *J. Am. Chem. Soc.* **2016**, *138*, 9720−9728.

(21) Chorkendorff, I.; Niemantsverdriet, J. W. *Concepts of modern Catalysis and Kinetics*, 2nd ed.; Wiley-VCH: Weinheim, Germany, 2007.

(22) For relevant catalytic reactions using a stoichiometric amount or excess of catalyst see for example: (a) Denmark, S. E.; Fu, J. On the Mechanism of Catalytic, Enantioselective Allylation of Aldehydes with Chlorosilanes and Chiral Lewis Bases. *J. Am. Chem. Soc.* **2000**, *122*, 12021−12022. (b) Hirano, K.; Biju, A. T.; Piel, I.; Glorius, F. N-Heterocyclic Carbene-Catalyzed Hydroacylation of Unactivated Double Bonds. *J. Am. Chem. Soc.* **2009**, *131*, 14190−14191. (c) Walter, S. M.; Kniep, F.; Herdtweck, E.; Huber, S. M. Halogen-Bond-Induced Activation of a Carbon−Heteroatom Bond. *Angew. Chem., Int. Ed.* **2011**, *50*, 7187−7191. (d) Jungbauer, S. H.; Huber, S. M. Cationic Multidentate Halogen-Bond Donors in Halide Abstraction Organocatalysis: Catalyst Optimization by Preorganization. *J. Am. Chem. Soc.* **2015**, *137*, 12110−12120.

(23) Bhaduri, S.; Mukesh, D. *Homogeneous Catalysis: Mechanism and Industrial Applications*, 2nd ed.; Wiley: Hoboken, NJ, 2014.

(24) (a) MacMillan, D. W. C. The Advent and Development of Organocatalysis. *Nature* **2008**, *455*, 304−308. (b) Albrecht, L.; Jiang, H.; Jorgensen, K. A. A Simple Recipe for Sophisticated Cocktails: Organocatalytic One-Pot Reactions—Concept, Nomenclature, and Future Perspectives. *Angew. Chem., Int. Ed.* **2011**, *50*, 8492−8509. (c) Ooi, T. Virtual Issue Posts on Organocatalysis: Design, Applications, and Diversity. *ACS Catal* **2015**, *5*, 6980−6988.

(25) Du, Z.; Shao, Z. Combining Transition Metal Catalysis and Organocatalysis − an Update. *Chem. Soc. Rev.* **2013**, *42*, 1337−1378.

(26) Catellani, M.; Motti, E.; Della Ca, N. Catalytic Sequential Reactions Involving Palladacycle-Directed Aryl Coupling Steps. *Acc. Chem. Res.* **2008**, *41*, 1512−1522.

(27) Wang, P.; Li, G.-C.; Jain, P.; Farmer, M. E.; He, J.; Shen, P.-X.; Yu, J.-Q. Ligand-Promoted meta-C−H Amination and Alkynylation. *J. Am. Chem. Soc.* **2016**, *138*, 14092−14099.

(28) Terao, J.; Ikumi, A.; Kuniyasu, H.; Kambe, N. Ni- or Cu-Catalyzed Cross-Coupling Reaction of Alkyl Fluorides with Grignard Reagents. *J. Am. Chem. Soc.* **2003**, *125*, 5646−5647.

(29) Terao, J.; Todo, H.; Shameem, A. B.; Kuniyasu, H.; Kambe, N. Copper-Catalyzed Cross-Coupling Reaction of Grignard Reagents with Primary-Alkyl Halides: Remarkable Effect of 1-Phenylpropyne. *Angew. Chem., Int. Ed.* **2007**, *46*, 2086−2089.

(30) (a) Carbó, J. J.; Crochet, P.; Esteruelas, M. A.; Jean, Y.; Lledós, A.; López, A. M.; Oñare, E. Two- and Four-Electron Alkyne Ligands in Osmium-Cyclopentadienyl Chemistry: Consequences of the $\pi_\perp \rightarrow$M Interaction. *Organometallics* **2002**, *21*, 305−314. (b) Barrio, P.; Esteruelas, M. A.; Oñate, E. Reactions of Elongated Dihydrogen-Osmium Complexes Containing Orthometalated Ketones with Alkynes: Hydride-Vinylidene-π-Alkyne versus Hydride-Osmacyclopropene. *Organometallics* **2003**, *22*, 2472−2485. (c) Bolaño, T.; Castarlenas, R.; Esteruelas, M. A.; Oñate, E. Assembly of an Allenylidene Ligand, a Terminal Alkyne, and an Acetonitrile Molecule: Formation of Osmacyclopentapyrrole Derivatives. *J. Am. Chem. Soc.* **2006**, *128*, 3965−3973.

(31) (a) Sini, G.; Eiseinstein, O.; Crabtree, R. Preferential C-Binding versus N-Binding in Imidazole Depends on the Metal Fragment Involved. *Inorg. Chem.* **2002**, *41*, 602−604. (b) Burling, S.; Mahon, M. F.; Powell, R. E.; Whittlesey, M. K.; Williams, J. M. J. Ruthenium Induced C-N Bond Activation of an N-Heterocyclic Carbene: Isolation of C- and N-Bound Tautomers. *J. Am. Chem. Soc.* **2006**, *128*, 13702−13703. (c) Wiedemann, S. H.; Lewis, J. C.; Ellman, J. A.; Bergman, R. G. Experimental and Computational Studies on the Mechanism of N-Heterocycle C-H Activation by Rh(I). *J. Am. Chem. Soc.* **2006**, *128*, 2452−2462. (d) Brill, M.; Díaz, J.; Huertos, M. A.; López, R.; Pérez, J.; Riera, L. Imidazole to NHC Rearrangements at Molybdenum Centers: An Experimental and Theoretical Study. *Chem. - Eur. J.* **2011**, *17*, 8584−8595.

(32) Liang, Q.; Salmon, A.; Jinhyung Kim, P.; Yan, L.; Song, D. Unusual Rearrangement of an N-Donor-Functionalized N-Heterocyclic Carbene Ligand on Group 8 Metals. *J. Am. Chem. Soc.* **2018**, *140*, 1263−1266.

(33) (a) Bruce, M. I. Organometallic Chemistry of Vinylidene and Related Unsaturated Carbenes. *Chem. Rev.* **1991**, *91*, 197−257. (b) Puerta, M. C.; Valerga, P. Ruthenium and Osmium Vinylidene Complexes and Some Related Compounds. *Coord. Chem. Rev.* **1999**, *193−195*, 977−1025. (c) Lynam, J. M. Recent Mechanistic and Synthetic Developments in the Chemistry of Transition-Metal Vinylidene Complexes. *Chem. - Eur. J.* **2010**, *16*, 8238−8247.

(34) (a) Buil, M. L.; Esteruelas, M. A.; Garcés, K.; Oñate, E. From Tetrahydroborate- to Aminoborylvinylidene-Osmium Complexes via Alkynyl-Aminoboryl Intermediates. *J. Am. Chem. Soc.* **2011**, *133*, 2250−2263. (b) Batuecas, M.; Escalante, L.; Esteruelas, M. A.; García-Yebra, C.; Oñate, E.; Saá, C. Dehydrative Cyclization of Alkynals: Vinylidene Complexes with the C_β Incorporated into Unsaturated Five- or Six-Membered Rings. *Angew. Chem., Int. Ed.* **2011**, *50*, 9712−9715. (c) Esteruelas, M. A.; López, A. M.; Mora, M.; Oñate, E. Reactions of Osmium−Pinacolboryl Complexes: Preparation of the First Vinylideneboronate Esters. *Organometallics* **2012**, *31*, 2965−2970. (d) Müller, A. L.; Wadepohl, H.; Gade, L. H. Bis(pyridylimino)-isoindolato (BPI) Osmium Complexes: Structural Chemistry and Reactivity. *Organometallics* **2015**, *34*, 2810−2818. (e) Wen, T. B.; Lee, K.-H.; Chen, J.; Hung, W. Y.; Bai, W.; Li, H.; Sung, H. H. Y.; Williams, I. D.; Lin, Z.; Jia, G. Preparation of Osmium η^3-Allenylcarbene

DOI: 10.1021/acs.organomet.8b00110
Organometallics XXXX, XXX, XXX−XXX

Complexes and Their Uses for the Syntheses of Osmabenzyne Complexes. *Organometallics* **2016**, *35*, 1514−1525. (f) Casanova, N.; Esteruelas, M. A.; Gulías, M.; Larramona, C.; Mascareñas, J. L.; Oñate, E. Amide-Directed Formation of Five-Coordinate Osmium Alkylidenes from Alkynes. *Organometallics* **2016**, *35*, 91−99.

(35) (a) Bolaño, T.; Castarlenas, R.; Esteruelas, M. A.; Modrego, F. J.; Oñate, E. Hydride-Alkenylcarbyne to Alkenylcarbene Transformation in Bisphosphine-Osmium Complexes. *J. Am. Chem. Soc.* **2005**, *127*, 11184−11195. (b) Bolaño, T.; Castarlenas, C.; Esteruelas, M. A.; Oñate, E. Nazarov Type Cyclization on an Osmium-Dienylcarbene Complex. *J. Am. Chem. Soc.* **2009**, *131*, 2064−2065.

(36) Danopoulos, A. A.; Tsoureas, N.; Green, J. C.; Hursthouse, M. B. Migratory Insertion in N-Heterocyclic Carbene Complexes of Palladium; an Experimental and DFT Study. *Chem. Commun.* **2003**, 756−757.

(37) Couzijn, E. P. A.; Zocher, E.; Bash, A.; Chen, P. Gas-Phase Energetics of Reductive Elimination from a Palladium(II) N-Heterocyclic Carbene Complex. *Chem. - Eur. J.* **2010**, *16*, 5408−5415.

(38) (a) Becker, E.; Stingl, V.; Dazinger, G.; Puchberger, M.; Mereiter, K.; Kirchner, K. Facile Migratory Insertion of a N-Heterocyclic Carbene into a Ruthenium-Carbon Double Bond: A New Type of Reaction of a NHC Ligand. *J. Am. Chem. Soc.* **2006**, *128*, 6572−6573. (b) Becker, E.; Stingl, V.; Dazinger, G.; Mereiter, K.; Kirchner, K. Migratory Insertion of Acetylene in N-Heterocyclic Carbene Complexes of Ruthenium: Formation of (Ruthenocenylmethyl)imidazolium Salts. *Organometallics* **2007**, *26*, 1531−1535. (c) Ma, C.; Ai, C.; Li, Z.; Li, B.; Song, H.; Xu, S.; Wang, B. Synthesis and Alkyne Insertion Reactions of NHC-Based Cyclometalated Ruthenium(II) Complexes. *Organometallics* **2014**, *33*, 5164−5172. (d) Hatanaka, T.; Ohki, Y.; Tatsumi, K. Coupling of an N-Heterocyclic Carbene on Iron with Alkynes to Form η^5-Cyclopentadienyl-Diimine Ligands. *Angew. Chem., Int. Ed.* **2014**, *53*, 2727−2729.

(39) (a) Santiago, A.; Gómez-Gallego, M.; Ramírez de Arellano, C.; Sierra, M. A. Structure and Photoreactivity of Stable Zwitterionic Group 6 Metal Allenyls. *Chem. Commun.* **2013**, *49*, 1112−1114. (b) Giner, E. A.; Santiago, A.; Gómez-Gallego, M.; Ramírez de Arellano, C.; Poulten, R. C.; Whittlesey, M. K.; Sierra, M. A. Mono- and Bimetallic Zwitterionic Chromium(0) and Tungsten(0) Allenyls. *Inorg. Chem.* **2015**, *54*, 5450−5461.

(40) Sierra, M. A.; Merinero, A. D.; Giner, E. A.; Gómez-Gallego, M.; Ramírez de Arellano, C. An Entry to Mixed NHC−Fischer Carbene Complexes and Zwitterionic Group 6 Metal Alkenyls. *Chem. - Eur. J.* **2016**, *22*, 13521−13531.

(41) (a) Bolaño, T.; Castarlenas, R.; Esteruelas, M. A.; Oñate, E. Assembly of an Allenylidene Ligand, a Terminal Alkyne, and an Acetonitrile Molecule: Formation of Osmacyclopentapyrrole Derivatives. *J. Am. Chem. Soc.* **2006**, *128*, 3965−3973. (b) Bajo, S.; Esteruelas, M. A.; López, A. M.; Oñate, E. Osmium-Acyl Decarbonylation Promoted by Tp-Mediated Allenylidene Abstraction: A New Role of the Tp Ligand. *Organometallics* **2014**, *33*, 4057−4066. (c) Toscani, A.; Marín-Hernández, C.; Moragues, M. E.; Sancerón, F.; Dingwall, P.; Brown, N. J.; Martínez-Máñez, R.; White, A. J. P.; Wilton-Ely, J. D. E. T. Ruthenium(II) and Osmium(II) Vinyl Complexes as Highly Sensitive and Selective Chromogenic and Fluorogenic Probes for the Sensing of Carbon Monoxide in Air. *Chem. - Eur. J.* **2015**, *21*, 14529−14538.

(42) Castarlenas, R.; Esteruelas, M. A.; Oñate, E. Δ^2- and Δ^3-Azaosmetine Complexes as Intermediates in the Stoichiometric Imination of Phenylacetylene with Oximes. *Organometallics* **2001**, *20*, 2294−2302.

(43) Blessing, R. H. An Empirical Correction for Absorption Anisotropy. *Acta Crystallogr., Sect. A: Found. Crystallogr.* **1995**, *51*, 33−38. *SADABS: Area-detector absorption correction*; Bruker-AXS, Madison, WI, 1996.

(44) *SHELXTL Package v. 6.14*; Bruker-AXS, Madison, WI, 2000. Sheldrick, G. M. A short history of SHELX. *Acta Crystallogr., Sect. A: Found. Crystallogr.* **2008**, *64*, 112−122.

(45) Sheldrick, G. M. *CELL NOW, program for unit cell determination*; University of Göttingen, Göttingen, Germany, 2005, and Bruker AXS, Madison, WI, 2005.

(46) Sheldrick, G. M. *Twinabs, Bruker AXS scaling for twinned crystals, version 2007/3*, and *Sadabs, Bruker AXS area detector scaling and absorption correction, version 2007/2*; University of Göttingen, Göttingen, Germany, 2007, and Bruker AXS, Madison, WI, 2007.

DOI: 10.1021/acs.organomet.8b00110
Organometallics XXXX, XXX, XXX−XXX